PAPERS IN PHYSICAL OCEANOGRAPHY AND METEOROLOGY

PUBLISHED BY

MASSACHUSETTS INSTITUTE OF TECHNOLOGY

AND

WOODS HOLE OCEANOGRAPHIC INSTITUTION

VOL. XII, No. 3

MEASUREMENTS OF THE VERTICAL WATER VAPOR TRANSPORT AND DISTRIBUTION WITHIN UNSTABLE ATMOSPHERIC GROUND LAYERS AND THE TURBULENT MASS EXCHANGE COEFFICIENT

BY

ANDREW F. BUNKER

Contribution No. 618 from the Woods Hole Oceanographic Institution

---

CAMBRIDGE AND WOODS HOLE, MASSACHUSETTS

DECEMBER, 1952

CONTENTS

ACKNOWLEDGMENTS

THE investigation described in this paper was conducted at the Woods Hole Oceanographic Institution with the support of the Office of Naval Research under Contract N6onr-27702 (NR-082-021).

All credit for the success of the observational part of the program is given to Kenneth McCasland who was either co-observer or sole observer on all airplane flights save two. The instruments were calibrated, installed in the airplane, and maintained almost exclusively by him. He designed, improved, or constructed many of the instruments used.

Bernhard Haurwitz, supervisor of the marine meteorology project, has aided the author both in the basic research and in the writing of this report. Others of the project who have aided in the instrumentation, reduction of data, and discussion of results, are Donald Parson Jr., Nellie Andersen, Betty Lou Geggatt, and Joanne S. Malkus.

Thanks are due to Marvin Odom, pilot and owner of the Stinson Voyager, for his skill and interest in flying the sounding helixes.

R. B. Montgomery helped in the initial planning of the project by making available airplane soundings obtained during the war years by the M.I.T. Radiation Laboratory, and by criticizing the present paper.

Given A. Brewer, manager of the Massachusetts Air Industries, helped the project by calibrating the response of the Lockheed Electra airplane to the turbulent gusts of air.

I. INTRODUCTION

1. *Evaporation and turbulent diffusion in an unstable air mass.*

The series of observations described in this report were planned with the double purpose of measuring the evaporation and transport of water vapor from the ocean into an unstable atmosphere, and of studying the diffusion processes operating in air of this stability class. Measured values of the evaporation from ocean surfaces were conspicuously absent from the meteorological literature until Craig and Montgomery (1949) published values for hydrostatically stable air. The present set of measurements extends our knowledge to include evaporation into a hydrostatically unstable air mass. In addition to evaporation values at the surface, net transports of water vapor at many levels up to 2000 meters have been measured.

Coefficients of the turbulent mass exchange have been computed at several heights from transport values and measured mixing ratio gradients. These computations show that the exchange coefficient can attain values over the wide range of 780 to 15,000 gm cm^{-1} sec^{-1}. Previously, the coefficient was measured under more stable conditions and values between 1 and 1000 gm cm^{-1} sec^{-1} were thought representative of most conditions encountered in the atmosphere. It is found that the coefficient may be three orders of magnitude larger in an unstable than in a very stable air mass, while a factor of five to one exists between the unstable class and a slightly stable class. The variation of the coefficient of turbulent mass exchange throughout the entire ground layer has been investigated. The coefficient is shown to increase rapidly in the first 100 m to a maximum value of about 2000 gm cm^{-1} sec^{-1}. From this level the turbulence dies slowly to a value of 100 gm cm^{-1} sec^{-1} at about 1500 m near the base of the temperature inversion at the top of the ground layer. In the inversion region turbulence is slight and the coefficient drops to between 1 and 10 gm cm^{-1} sec^{-1}.

The analysis on the basis of the coefficient of turbulent mass exchange is not a complete one, since it does not consider the effects of free-convection, which is always present or incipient in an unstable air mass. An approximate evaluation of the magnitude and transport by convection has been made on the basis of available information concerning the frequency of convection parcels, their velocities, and water vapor content. The final description of the processes operating in an unstable layer of air is not reached in this paper but must be worked out in terms of buoyant parcels or jets rising through highly turbulent regions of the atmosphere. The buoyancy forces of the parcels may be dissipated rapidly by the effects of entrainment and diffusion of the outside air, so that only under very critical conditions can convection become fully developed.

The observing techniques were modelled after the meteorological work of the Radiation Laboratory of Massachusetts Institute of Technology. Their technique of flying psychrograph equipped airplanes in helical soundings was successfully adapted to the needs of the present study. In addition to the thermistor aero-psychrograph, the airplane usually carried a water-column accelerometer which recorded the vertical accelerations imparted to the sounding aircraft by the turbulent gusts.

The temperature and roughness observations were continued upward through the inversion existing at the top of the ground layer of air and extended a hundred meters or so into the smooth air above the inversion. Particular attention has been concentrated in this paper on the 30 m to 2000 m region, which is not easily observable by ground-, boat-, or tower-based instruments, and has been neglected in the past. The observing procedure was organized so that the two quantities, mixing ratio gradient and vertical flow of water vapor, could be determined with sufficient accuracy to yield significant values of the coefficient of turbulent mass exchange. Accuracy in the vertical gradient determination was achieved by executing slow ascents with the airplane, thereby eliminating errors due to the lag of the psychrograph thermistors. Accuracy in the determination of the vertical flow of water vapor was attained by measuring the mixing ratios in areas sufficiently separated downwind to assure that the observed mixing ratio increases were much greater than the probable errors of the mixing ratio determination.

Air masses moving from land out over the water were followed by the sounding airplane. From two

or more soundings, accumulations of water vapor in the downwind air were obtained and rates of transport determined. Dry- and wet-bulb temperature, or dry-bulb and dew-point temperatures were recorded alternately every five seconds, while the plane made helical ascents. The slow ascent of the plane, 60 m per minute, allowed the accurate measurement of the mixing ratio gradient throughout the layer.

The computed values of the vertical flow of water vapor and mixing ratio gradients have been placed in the eddy diffusion equation,

$$E_z = -A_z \frac{\partial q}{\partial z} \qquad (1)$$

to obtain values of A_z, the coefficient of turbulent mass exchange. The value of A_z as determined from the original observations, includes any influence of convection that may be present in the atmosphere. Since both large convection currents and "convective turbulence", as defined by Priestley and Swinbank (1947) will modify the value of A_z descriptive of eddy diffusion alone, it is logical to re-define A_z by equation (1), rather than by a definition based on the statistical treatment of small scale eddies. By this change, A_z is made to describe the state of mixing of the atmosphere as it actually exists, regardless of the process creating the turbulence or mass exchange. The analysis in Section IV, 1, is made with this definition of the coefficient. In Section IV, 3, a separation of the transport by diffusion and convection is accomplished.

Indirect methods of determining the rates of evaporation or transport of water vapor from land and water surfaces have been devised and used by numerous workers since Dalton (1802) established the relation between evaporation and the difference between aqueous vapor pressure in the air in contact with the water and in the air at a higher level. Sverdrup (1936, 1937), Montgomery (1940), Thornthwaite and Holzman (1942), and others, have used moisture and wind gradients in conjunction with theoretical turbulence relations, such as are summarized and developed more completely by Dryden (1943), to obtain expressions for the evaporation or transport in the atmosphere.

The evaporation and transport have been studied directly by several workers by observing modification of air masses. Lettau (1937) obtained observations from free balloon flights. Radiosonde data were studied by Petterssen (1940). Burke (1945) studied air mass modifications from weather maps, radiosonde, and ship reports, developing charts for use as forecasting aids. Craig (1949) studied airplane soundings taken over water surfaces to determine the eddy diffusion of water vapor in stable air.

2. *The ground layer and its inversion.*

a. Nomenclature.

The lower layers of the atmosphere studied in this work have received a confusing number of names from previous workers in the field. Some names are based on processes operating in the air: e.g., *turbulent layer*, *convective layer*, and *layer of frictional influence*. Others are based on properties of the layer: e.g., *homogeneous layer*, *mixed layer*, and *unstable layer*.

The notation *ground layer*, as defined by Flohn and Penndorf (1950) seems best suited for the general case, and is adopted in the present report. The layer has been subdivided into three regions: a *bottom frictional region* defined by an increase in the value of the coefficient of turbulent mass exchange, an *upper frictional region* defined by a decrease in the coefficient, and a third region, called *peplopause* by Schneider-Carius (1947), but here designated as the *inversion region*. The ground layer, continuing with the Flohn and Penndorf nomenclature, is bounded below by the two meter stratum, called the *bottom layer*, and above by the *advection layer*.

The normal type ground layer (Schneider-Carius, 1947a) has been studied exclusively in the present work. Figure 1 has been drawn to show the main features of the normal type ground layer and to identify and compare the regions studied by authors using different nomenclature. Schematic temperature, mixing ratio, and exchange coefficient curves are shown with frequently occurring height ranges of a few significant boundaries. The well-developed, normal type ground layer is identified more easily by the approximately dry-adiabatic temperature lapse rate and small mixing ratio lapse rate (10^{-9} cm^{-1}) than by the defining height variation of the wind. This is particularly true at the upper boundary where the upper frictional region is topped by the turbulence inversion.

b. The inversion region.

The low values of the turbulent mass exchange coefficient in the inversion cause the great decrease

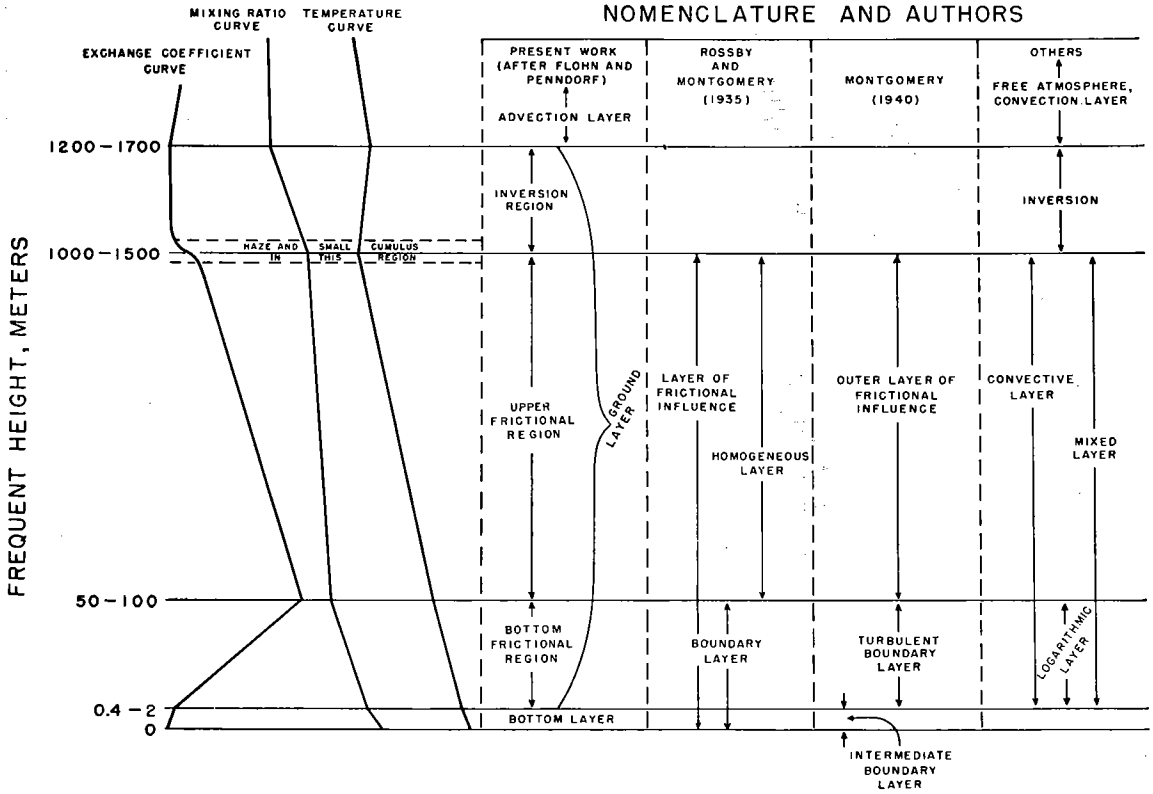

FIG. 1. Schematic vertical distribution of properties throughout the ground layer, and nomenclature of the subdivisions of the ground layer.

in the mixing ratio value that frequently is encountered in passing from the upper frictional region into the inversion. The sharpness of the boundary is shown by the potentiometer records of a test airplane flight with a humidity strip on January 5, 1951. Figure 2, a photograph of part of the record, shows a relative humidity decrease from 60% to 25% in a height interval of but 120 m.

The base of the temperature inversion may be observed visually from an airplane on many occasions through the development of a haze-layer. This phenomenon occurs whenever the inversion is strong, and relative humidities above 60–70% are created in the top of the upper region of the ground layer. Condensation of water vapor on the hygroscopic nuclei present in the air cause considerable absorption and scattering of light in a relatively thin layer of air. Figure 3, a photograph taken from an airplane flying at the level of the haze-layer, shows the dark band created by the absorption and scattering of light by distant water drops. Scattering of sunlight by drops nearer the plane produces a whitish light extending several degrees above and below the dark band. The effect is much more pronounced to the eye or on color film than on a black and white photograph, and is a great aid to an observer wishing to locate the top of the upper region of frictional influence.

The property of small transport between the ground layer and the advection layer, whenever separated by a strong inversion, has been used in the present work in the determination of the flow of water vapor into the atmosphere.

The magnitude of the flow of water vapor through the inversion during a polar outbreak has been investigated by the author (1950)[1] in an unpublished report, following the techniques of Hewson (1936, 1938). Radiosonde observations of the Weather Bureau were used as the source of humidity values. Two outflows of cPk air masses were followed from the Dakota-Montana region to the east coast. The increase in moisture above

[1] A. F. Bunker. Woods Hole Oceanographic Institution, Reference No. 50–21. Manuscript report to the Office of Naval Research.

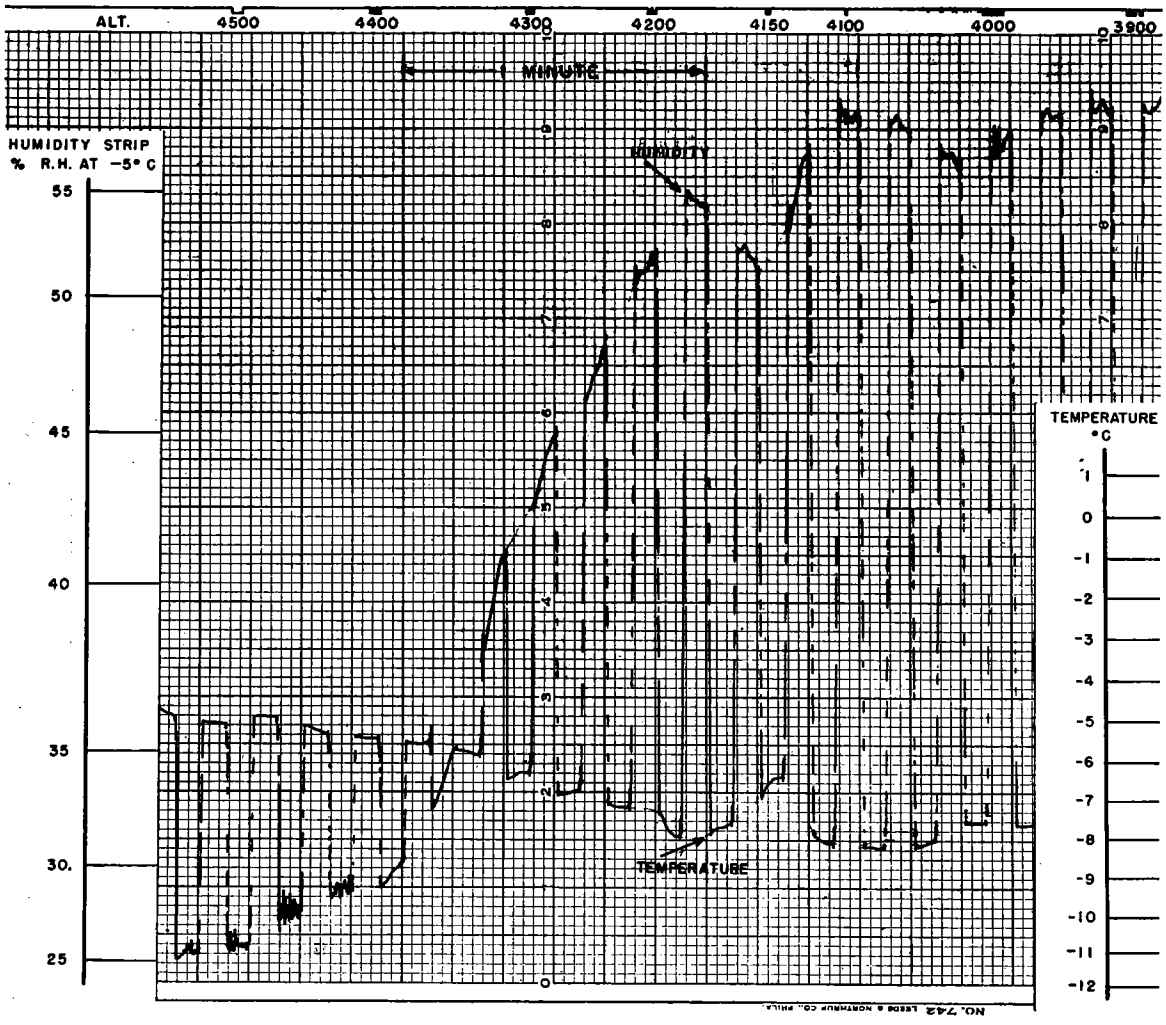

FIG. 2. Rapid humidity decrease through inversion base recorded during test flight January 5, 1951, with a radiosonde humidity strip adapted for airplane soundings.

the inversion during the passage of the air was noted. Flows through the base of the inversion were determined to lie between 1×10^{-7} to 10×10^{-7} gm cm^{-2} sec^{-1} $\pm$ 2×10^{-7} gm cm^{-2} sec^{-1}. The coefficient of turbulent mass exchange varied between 80 and 140 gm^{-1} cm^{-1} sec^{-1} $\pm$ 75 gm cm^{-1} sec^{-1}. The values of the flow and the coefficient at the top of the inversion vary from 1×10^{-8} to 10×10^{-8} gm cm^{-2} sec^{-1} $\pm$ 11×10^{-8}, and from 14 to 26 gm cm^{-1} sec^{-1} $\pm$ 100 gm cm^{-1} sec^{-1}. As these probable errors are large, it is planned to recheck these values with airplane observations in place of the radiosonde observations. Taking into account the large probable errors, it is proven that a probable maximum of only 21×10^{-8} gm cm^{-2} sec^{-1}, or roughly 1.5% of the surface flow, diffuses through the top of the inversion. The average flow will be much less than this possible maximum flow.

The decision to use the ground layer inversion as a meteorological tool in the study of evaporation and water vapor flow by eddy diffusion was made after a brief study for this purpose of airplane soundings taken during the war years by the M.I.T. Radiation Laboratory. No reliable values were found since the soundings extended to only 1000 feet, while water vapor was transported to higher levels in cases of an unstable layer. This limitation prevented the determination of the total amount of water vapor transported and stored in the atmosphere. An approximate value could be found by using the lowest inversion shown by

FIG. 3. Layer of haze photographed from an airplane flying overland at the inversion base level on February 3, 1950. Air to ground visibility below haze was better than 50 km.

radiosonde observations taken in the region. The values determined from the study of the M.I.T. data have never been published, but agree quite well with values found in the present investigation. The study of these data was invaluable in that it pointed out the need of continuing the airplane soundings up through the inversion region.

It should be pointed out, however, that this negligibly small transport through the inversion is not a general property of the upper boundary of the ground layer, but rather is an infrequent occurrence. An inversion capable of severely limiting transport develops in a cP air mass only when the air aloft is quite stable and subsidence occurs in the air mass as it travels out of the polar regions. At other times, and in other geographical regions, considerable amounts of water vapor are transported through the ordinarily weak inversion or stable region. In fact, the entire hydrological cycle of water vapor through the atmosphere depends on easy passage through this boundary layer.

Cumulus clouds occasionally developed in the ground layer studied in this report, but rarely broke through the inversion into the air aloft. Instead, the clouds came to rest after penetrating only 100 or 200 meters of the inversion air, then fell back into the turbulent air.

Figure 4 is a photograph of the clouds over the Gulf of Maine, February 3, 1950. Their small vertical development and uniform tops are the result of the rapid damping by the strong inversion and demonstrate that, at least on this particular day, no moisture escaped by convection into the upper air.

3. *Geographic areas and synoptic situation studied.*

The coastal water of New England served as the warm water surface for the study of diffusion

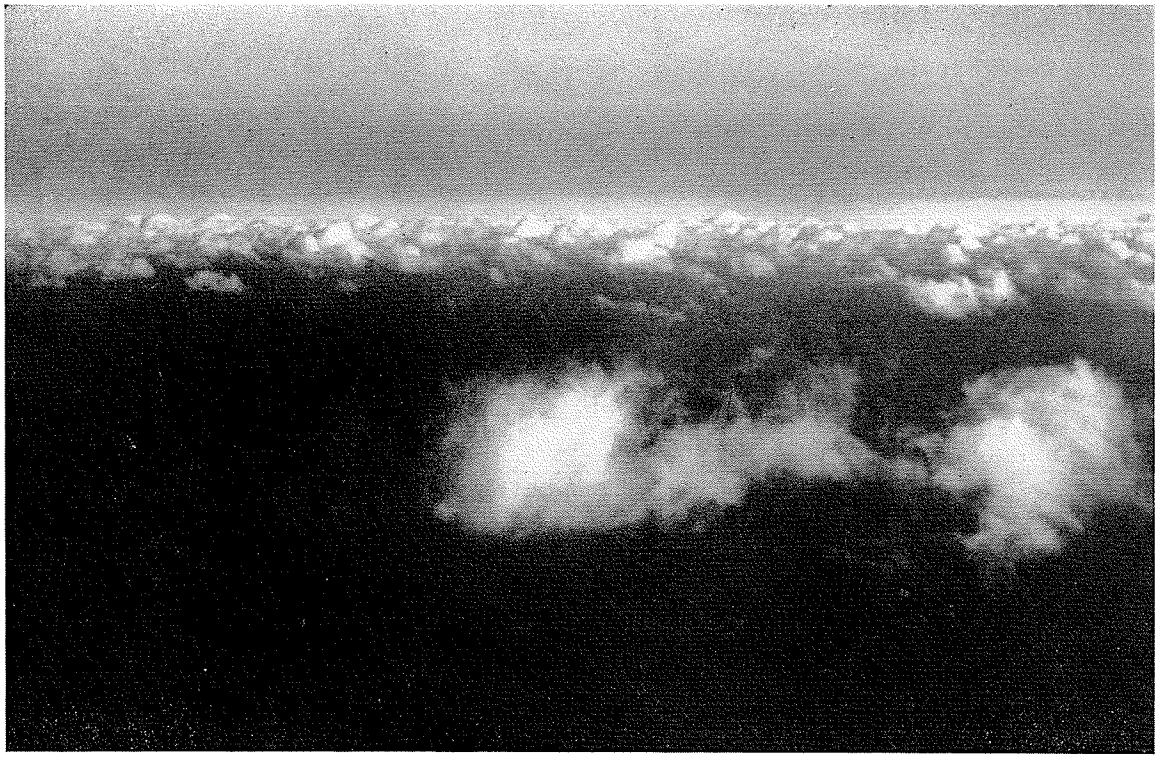

FIG. 4. Clouds and haze layer photographed over the Gulf of Maine, February 3, 1950, at 2000 m.

of water vapor into continental air masses. Most of the series of observations were made in the Buzzards Bay-Vineyard Sound area of southeastern Massachusetts. Over-water trajectories up to 35 km long were studied in the area during the falls and winters of 1947–48 and 1948–49. Longer trajectories up to 150 km long were studied during the winter of 1949–50 over the Gulf of Maine. The irregular coast of Massachusetts was suitable for the work, since it offered both open fetches of water and nearby islands or lightships required for the safety of small planes. The Gulf of Maine likewise was ideal for the study of diffusion when larger two-engined planes were used.

The desired weather situation was the post-cold-frontal outflow of continental air. Time was allowed for the front to move far out to sea so that the frontal surface aloft would not interfere with the development of the ground layer. Under these circumstances, a fully developed ground layer, complete with capping inversion, moved over the warmer water.

Conditions of neutral equilibrium or thermal instability in the ground layer are treated in the present paper. Observations were carried out when both the land and water surfaces were warmer than the air in contact with them.

The one exception to this condition is the series of September 15, 1948. In this case an unstable air mass became slightly stable by passing over water that was 0.8°C cooler than the air. The series was not excluded from this report since vigorous turbulent mixing continued to the base of the inversion. In constrast, a series obtained October 13, 1948, was excluded because the water was 2° cooler than the air, and turbulent mixing was confined to the lowest 50 m during a large part of the passage of the air over the water.

During the three fall-winter periods of observations twenty-five flights were completed. The results of only fifteen of these flights are reported in the present paper. Reasons for the exclusion from this report, or the complete discard of the data of certain flights, are enumerated below.

Six complete sets were discarded due to the failure of the humidity measuring equipment. Four of these failures, in the winter of 1947–48,

were caused by the freezing and thawing of the wetted wick. One resulted from the failure of an experimental heated psychrograph to give mixing ratio values sufficiently reliable for diffusion study. The dew-point recorder failed on one flight.

Two sets of data, that taken October 13, 1948, and one taken November 22, 1949, were not reported because of adverse meteorological conditions. On the latter date, an over-riding of the continental air by a maritime air mass caused 10/10 stratocumulus with moderate icing and a consequent masking of diffusion effects.

Two other sets of data are not included here, but will be the basis of a future study on the modification of the ground layer by cooling, heating, and land masses.

II. INSTRUMENTS AND OBSERVATIONAL PROCEDURE

1. *Airplane, boat, and ground equipment.*

a. Psychrograph.

The first temperature-measuring instrument used in this investigation was an airplane psychrograph designed and built by the Radiation Laboratory of the Massachusetts Institute of Technology. This psychrograph has been described by Katz (1947). It is sufficient to say that it records alternately, on an Esterline-Angus recording milliammeter, currents proportional to the dry- and wet-bulb temperatures. The thermal lag of the resistor elements is 4 seconds, with a ventilation speed of 100 knots.

A modification of the psychrograph was used after the summer of 1949. This later psychrograph bridge designed and built by McCasland applies only a half volt across the resistor, thus reducing internal heating. The thermistor resistance records on a Leeds and Northrup potentiometer. The power-driven pen of the potentiometer is ideally suited for operation in airplanes or boats, since it is unaffected by pitch, yaw, roll or vibration.

The radiation shield containing the temperature sensitive elements was mounted on a wing strut or mast protruding from the nose-piece of the airplane (see Figure 5). The amplifier, recorder, batteries, and the vibrator which converts the 6V direct current into the 110V alternating current, were placed on the plane's back seat and floor.

During the winter of 1948–49 the atmosphere was sounded with an experimental psychrograph equipped with an electric heater, which preheated the air before passing over the thermal elements. The purpose was to extend the use of the psychrograph to sub-freezing temperatures. This psychrograph was found to be too inaccurate for diffusion studies.

A psychrograph similar to the one already described was mounted in the cabin of a boat so that soundings could be made from a meter or so above the water up to a height of one hundred meters. Two amplifiers and recorders were constructed so that simultaneous readings of dry- and wet-bulb temperature could be recorded. The dry- and wet-bulb thermistor elements were mounted in an aluminum housing for radiation shielding. The housing and connecting wires were lifted by a 1000 gm hydrogen-filled captive balloon. Values were obtained in the lowest few meters over the water by attaching the housing to a pole, and guiding the housing over the waves. Difficulties were experienced with moisture in switches, and breakdown of electrical insulation in the connecting wires. Only one set of soundings was obtained which was free from insulation breakdown.

b. Dew-point recorder.

The automatic dew-point recorder, manufactured by Gibbs Co., was used during the winter of 1949–50, for work over the Gulf of Maine. Outside air was supplied to the mirror by a hose attached to the fresh-air intake of the plane, after a check up showed that no contamination of the air occurred. Dry ice (solid CO_2) and alcohol were used as a coolant for the mirror and as a reference bath for the thermocouple. The thermocouple voltage was recorded on a Leeds and Northrup Speedomax potentiometer, which intermittently recorded the dew-point signal and the dry-bulb temperature signal from a thermistor element mounted in the nose-piece, as already

FIG. 5. Psychrograph housing being mounted on wing strut by Kenneth McCasland, observer, and Marvin Odum, pilot. Amplifier and power supply are on the ground.

described. A mercury in glass thermometer was used to determine the temperature of the reference bath.

c. Accelerometer.

A water-column accelerometer was carried by the sounding aircraft after the summer of 1948.

This instrument records the vertical accelerations imparted to the airplane by the turbulence of the air. The unit was placed on the cabin floor as close to the main wing spar as possible.

d. Other airplane equipment and instruments.

A push button and relays were arranged to move pens at the side of the recording paper so that simultaneous marks could be made on both the temperature traces and the accelerometer traces. Times, altitudes, entry into clouds, and other occurrences were entered in code on the side of the traces by the observer.

The plane's altimeter, essentially an aneroid barometer, an airspeed indicator, and a pitot tube, were used exclusively for altitude and speed information.

A sling psychrometer was carried as a check on the operation of the electronic instruments. It could be used conveniently from the airplane window or fresh-air intake.

A camera was available in the plane for cloud and haze layer pictures.

e. Sounding airplanes.

The airplane most frequently flown was the Stinson Voyager. It was used for all the flying in the Buzzards Bay region from June, 1947, until the beginning of the work over the Gulf of Maine in the fall of 1949. This single-engined, four-place airplane could carry the pilot, one observer, the amplifier, accelerometer, vibrator, and battery. The observer sat in the right front seat where he could see the altimeter and airspeed indicator and service the instruments behind him in the back seats.

One trip over the Gulf of Maine was made in a twin-engined Cessna, but this plane was discarded since it would not maintain altitude on one engine with the pilot, observer, and equipment. The work over the Gulf of Maine was continued in a twin-engined Lockheed Electra and a DC-3. These planes have ample room and lift for the power supply necessary for the dew-point recorder, and allowed two observers to make the flights.

f. Bathythermograph.

Water temperatures were taken both by dip bucket and by bathythermograph. The bathythermograph, which records water temperature against depth on a smoked glass slide, has been described by Spilhaus (1938).

g. Land station equipment.

Observations were made from the Woods Hole dock of the winds aloft, surface winds, pressure and water temperatures. Pilot balloon observations were carried out in the usual manner except that 30-second readings were taken. A few double theodolite observations were made.

Supplementary weather information, including surface maps, hourly data, radiosonde observations, and winds aloft, were obtained from the M.I.T. terminal of the U. S. Weather Bureau teletype circuit, or the Daily Upper Air Bulletin.

2. *Sounding procedures.*

The first step in the day's work was to determine the present wind and check with the wind forecast as broadcast by the U. S. Weather Bureau. The winds aloft were computed from the pilot balloon observation taken early in the morning. From these, and any changes in wind direction mentioned in the forecast, a probable trajectory of air moving offshore was determined. A distance interval downstream between soundings was decided upon so that measurements would be made in nearly the same air, thus reducing any advection effects that might be present. A series of observation points was located that satisfied the trajectory of the air, the proper spacing of the soundings, and that allowed the single-engined plane to circle near an island or lightship for safety.

Upon the arrival of the airplane at the selected spot overland a 500 meter radius helical ascent was started from about a 50 m altitude. The pilot attempted to maintain a 70 knot air speed and a 200 foot per minute climb. The observer made altitude check marks on the recorder paper and kept a log of altitude, air speed, roughness, cloud amounts, etc. The ascent was continued until it was noticed, either from the psychrograph record, or from the sudden entry into the smooth air above the turbulent layer, that the inversion at the top of the ground layer was reached. The climb was continued another 100 meters before leaving the location for the next downwind sounding area. Here the same procedure was repeated, except that the plane was flown much closer to the water than to the land surface. Each series

of observations consisted of two to four soundings. Figure 6 is a photograph of a U. S. Coast and Geodetic Survey chart, showing an area frequently used for soundings. Wire springs of the proper diameter were cut at the correct height to depict the 500 meter radius helix made by the airplane as it climbed to the top of the ground layer.

out the observations over the Gulf of Maine. A series of three soundings was flown; one overland, one 20 km or so downwind, and the last at either 42°35′N, 69°00′W or 42°35′N, 69°30′W. The position 42°35′N, 69°00′W has the invaluable property of being equidistant from points on the coast from Duxbury, Massachusetts, to Portland,

FIG. 6. Photograph of chart with springs representing the height, diameter, and relative positions of the helixes described by the sounding aircraft. The arrow indicates the average wind direction and distances expressed in kilometers.

The second observer either remained on the Institution dock, making wind aloft and water temperature observations, or proceeded to the sounding area with a boat equipped with a balloon borne psychrograph and bathythermograph. With these instruments water temperatures were obtained from the bottom of the bay or sound to the surface, and wet- and dry-bulb temperatures were obtained from 1 meter above the surface to 100 meters.

A similar procedure was followed in carrying

Maine. Any uncertainty in the direction of the wind has a negligible effect on the distance travelled over water, thus minimizing one of the many possible sources of errors.

Water temperatures near the sounding areas in the Gulf of Maine were observed on only two dates, November 7, 1949, and February 10, 1950. Probable water temperatures in the area on the desired days were found by interpolation with the aid of mean temperature charts on file at the Institution.

III. TABULATION AND DISCUSSION OF DATA

1. *Reduction of data to meteorological quantities.*

Methods of reducing the recorded output of the psychrograph and dew-point recorder to the desired meteorological quantities were devised which determined these quantities rapidly, and at the same time assured that no fictitious gradients or fluxes were introduced by approximations. Since over 600 computations were required for the average sounding, nomograms and special slide rules were constructed to facilitate the reduction of the data.

The values observed during the ascents of the airplane from which the quantitites are computed are: (1) the milliammeter or potentiometer reading of the dry- and wet-bulb resistances or dew-point voltages; (2) the indicated air speed, and (3) the altimeter reading.

a. Dry-bulb, wet-bulb, and dew-point temperatures.

The milliammeter or potentiometer readings were reduced to dry-bulb and wet-bulb temperatures by using tables made from laboratory calibrations of the temperature elements. The temperature-resistance calibrations of these elements were checked every few months before and during the observing periods. Most of the thermistors retained their calibration over long periods. A few drifted several tenths of a degree in a year's time. Pairs of thermistors were selected for the psychrograph on the basis of the stability of their calibrations. Dew-point temperatures were determined from the potentiometer reading of the dew-point recorder's thermocouple voltage and from the temperature of the reference bath.

Corrections had to be applied to the dry- and wet-bulb temperatures because of the heating caused by the compression of the air ahead of the moving elements. These were determined from the following equation given by AAF Weather Service (1945):

$$\Delta T = a_d(V/100)^2 \qquad (2)$$

Here a_d is a factor to be found experimentally for any particular psychrograph by flying at several speeds under a stratus overcast. Its value is 0.9 for the psychrographs used in the present work. The symbol V denotes the true air speed of the plane in miles per hour. The true air speed was found from the indicated air speed, and the altitude by use of an aircraft navigational plotting board. The equation gives the correction for the dry-bulb temperature. The wet-bulb correction may be found by multiplying the dry-bulb correction by the ratio of the saturation- and dry-adiabatic lapse rates.

b. Pressure.

The atmospheric pressure at each height, indicated by the plane's pressure altimeter, was read from an expanded table of the pressure-height relation of the standard atmosphere. This value was corrected by the surface pressure reading interpolated from the published Daily Weather Map of the U. S. Weather Bureau.

c. Mixing ratio.

The mixing ratio, w, was computed from the following form of the psychrometric equation:

$$w = w_s - \frac{(T_d - T_w)\,(c_{pd} + wc_{pv})}{L} \qquad (3)$$

In this equation T_d and T_w are the dry- and wet-bulb temperatures, w_s is the saturation mixing ratio at the given wet-bulb temperature and pressure, c_{pd} and c_{pv} are the specific heats at constant pressure of dry air and water vapor respectively, and L, the heat of vaporization of water. The saturation mixing ratio was read from a large pressure-wet-bulb temperature diagram with isograms of mixing ratio drawn upon it. Four slide rules were constructed for the rapid determination of $(T_d - T_w)\,(c_{pd} + wc_{pv})/L$. For a frozen wick, values of the saturation mixing ratio over ice were computed from Table 78 of the Smithsonian Meteorological Tables (1939). The heat of sublimation was used in place of the heat of vaporization for the case of the frozen wick. Mixing ratios were found from the frost-point temperatures by entering a pressure-temperature diagram with mixing ratio isograms based on saturation with respect to water drawn upon it. Saturation mixing ratios so determined were converted to the mixing ratio of the air by means of a table converting relative humidity with respect to ice to relative humidity with respect to water.

d. Equivalent, virtual, potential temperature and height.

Nomograms were constructed to speed the computation of the equivalent, virtual, virtual potential, and dry-bulb potential temperatures. All potential temperatures are computed to the base 1000 mb. For comparison with the potential temperatures of the air column, surface water temperatures were reduced to potential temperatures, base 1000 mb, as though they were air temperatures.

True heights in meters were computed with the aid of a table and a graph from the average virtual temperature of a layer for a few selected pressures. All other heights were found graphically from the resulting pressure height relation.

2. *Probable errors of the observed and computed quantities.*

The probable errors associated with the calibration, measurement, reduction, and dynamic correction of the temperatures obtained with the M.I.T. psychrograph have been discussed previously by Bunker, et al (1949). Since the same psychrograph, or roughly similar ones, and the same method of data reduction were used in the present investigation, the same probable error of $\pm$ 0.23°C absolute error, or $\pm$ 0.10°C relative error within a given series of measurements will be used here. Likewise, since the same type of commercial airplane altimeter was installed in the airplanes, the probable error of a single altitude determination is accepted as $\pm$ 8 m (25 feet).

Combining the absolute probable error of the temperature and the error of the altitude (pressure), the probable error of a single mixing ratio determination in an air mass at about 0°C turns out to be $\pm$ 0.1 gm/kg. Since about 50 observations of the mixing ratio are made per sounding, the average mixing ratio of an air column is determined with a probable error of $\pm$ 0.014 gm/kg. This value was computed in such a manner as to imply a new zero setting of the psychrograph amplifier for each mixing ratio determination. In practice, the zero setting was left untouched, but any drift was noted at frequent intervals during the series of soundings. As the drift was always small, one particular value of the zero setting was applied to many determinations of the mixing ratio, so the probable error mentioned above is a fair determination of the error. Since the average mixing ratio of an air column usually changes several tenths of a gram per kilogram in traversing 10 km of water, the present method of observation is considered sufficiently accurate for the diffusion work at hand.

The probable error of a single pilot balloon observation in the lowest few kilometers is ascribed by Middleton (1942) to be $\pm$ 1 m/sec. The probable error of the average wind of the ground layer, based on ten individual values, is then $\pm$ 0.3 m/sec. The probable error so determined describes only the accuracy of measurement and not the accuracy with which the measurement describes the existing wind. If more than one ascent is averaged, the error will be correspondingly less than this value. In terms of time of transit over a distance of 10 km, a ground layer moving 10 m/sec would require 1000 $\pm$ 30 seconds to traverse the distance. The probable error of the flow determination can be found from the errors of determining the differences in mixing ratio between two columns and the errors of the transit times. For a flow equal to 5×10^{-5} gm cm^{-2} sec^{-1} and determined over a 10 km base line, the probable error equals $\pm 0.25 \times 10^{-5}$ gm cm^{-2} sec^{-1}. For a flow equal to 5×10^{-6} gm cm^{-2} sec^{-1} the error is $\pm 2 \times 10^{-6}$ gm cm^{-2} sec^{-1}. Determined over a 100 km base line, a flow equal to 5×10^{-6} gm cm^{-2} sec^{-1} will have an error of $\pm 0.25 \times 10^{-6}$ gm cm^{-2} sec^{-1}.

Using the previously discussed values of the probable errors of the mixing ratio and of the height measurements and 50 individual observations, it can be shown that a gradient determined to be 10^{-8} cm^{-1} will have an associated probable error of $\pm 10^{-9}$ cm^{-1}.

The determination o the coefficient of turbuflent mass exchange will have probable errors which depend primarily on the probable errors of the flow. For example, the coefficient based on a flow of $5 \times 10^{-5} \pm 0.25 \times 10^{-5}$ gm cm^{-2} sec^{-1} may be 1000 $\pm$ 100 gm cm^{-1} sec^{-1} while a coefficient based on a flow of $5 \times 10^{-6} \pm 2 \times 10^{-6}$ gm cm^{-2} sec^{-1} may be 1000 $\pm$ 400 gm cm^{-1} sec^{-1}. Thus it is seen that the errors in the coefficient computation may vary from $\pm$ 10% to $\pm$ 40% of the total value.

These values of the probable errors of the flux are based on the assumption that the atmospheric circulation corresponded perfectly to the measurements, within the probable error limits. Also, it

is assumed that no other processes were operating that might oppose or contribute to the moisture increase of the air. In fact, neither assumption is always true. Several cases of wind shift occurred during the observing program, making necessary the abandoning of the day's work. Wind shifts of a local or temporary character may have gone undetected on other days and led to actual errors greater than the computed probable errors. Phenomena such as lateral mixing, convection and convective break-through of the inversion, and local lee shore subsidence, all add an element of uncertainty to the flux determination. November 16, 1948, is an example of a possible depression of the measured flux value due to the lateral mixing. On this day the wind blew from a more northerly direction than expected (see Figure 8), so that mixing between the modified air over the Bay and unmodified air over the land could occur. A rough calculation of the lateral flow of water vapor, based on the estimated horizontal gradient and the calculated vertical exchange coefficient, shows that in the vicinity of the final sounding 9% of the water vapor passing through a unit horizontal surface diffuses laterally to the air over the land. Assuming an average of 4.5% during the passage of the air down the Bay, the true surface flow would be 40×10^{-7} gm cm^{-2} sec^{-1}, rather than the 38×10^{-7} entered in Table III. Errors due to other phenomena are harder to evaluate and may not be so fortunately low.

3. *Supplementary observations.*

Table I has been compiled to present supplementary observations taken during the days selected for the airplane psychrograph observations. The values entered here are averages for the period of observation, and are not necessarily characteristic of the entire day. The column headed "Pressure" gives the atmospheric pressure as measured with a mercurial barometer or determined from the weather map. The column labelled "Sky Conditions" describes the amount and type of low cloud present in the sounding areas at the time of observation. Data were taken from the airplane observer's notes. The "Wind Direction" and "Wind Speed" presented in the table is the average for the ground layer as determined from pilot balloon runs and surface data. Directions are in degrees, while speeds are expressed in meters per second. The water temperatures listed were obtained as follows: (1) by a dip bucket thermometer used either at a dock or from a boat, in or near the sounding area; (2) by a bathythermograph in the sounding area; (3) by comparison with mean charts on file at the Institution. The saturation mixing ratio of the air in contact with the water surface is given in the last column. It was computed from the water temperature and the surface pressure. The mixing ratio value entered in the next column is the average for the ground layer, exclusive of the

TABLE I

SUPPLEMENTARY OBSERVATIONS

Series Number	Date	Time EST	Atmospheric Pressure mb	Sky Conditions	Wind Direction Degrees	Wind Speed m/s	Water Temperature °C	Saturation Mixing Ratio gm/kg	Orig. Aver. Mixing Ratio gm/kg
1	9/1/48	1232–1410	1019	2/10 cumulus	340	11.0	18.8	13.1	5.5
2	9/15/48	1345–1552	1025	5/10 over mainld. nil over water	280 320	4.8* 6.4†	17.8	12.8	4.4
3	9/16/48	1155–1346	1032	3/10 cumulus	360	7.7	17.7	12.5	3.2
4	9/22/48	1105–1305	1008	No low cloud	315	6.5	17.3	12.4	4.0
5	9/23/47	1345–1515	1026	No low cloud	310	2.3	19.9	14.5	3.1
6	10/1/47	1112–1311	1025	No low cloud	315	7.3	16.6	11.7	2.2
7	10/20/49	1158–1310	1016	No low cloud	010	10.3	13.0	9.3	4.3
8	11/9/47	1520–1644	1007	5/10 stratus	290	8.2	12.2	9.0	2.6
9	11/10/47	1337–1432	1020	No low cloud	305	10.0	12.2	8.8	2.5
10	11/13/47	1450–1602	1013	5/10 cumulus	305	15.2	10.8	8.0	2.6
11	11/16/48	1145–1301	1029	5/10 over land No low cloud over water	005	4.8	8.5	6.9	3.0
12	11/17/47	1405–1557	1011	5/10 cumulus	310	13.7	8.6	7.0	2.7
13	12/30/49	1400–1540	1027	No low cloud	340	18.0	6.5–8.6	6.0–6.9	1.0
14	1/17/50	1415–1610	1029	0–5/10 cumulus	295	15.0	5.5–7.6	5.5–6.5	1.1
15	2/3/50	1358–1605	1006	0–3/10 cumulus	310	13.0	4.5–6.5	5.2–6.0	1.1

* 0–700 m † 700–2100 m

inversion region, of the unmodified air before it passed over the water surface.

4. *Discussion of four sample series of observations.*

Potential temperatures and mixing ratios observed on four days are plotted against height to show a few structural features that the ground layer frequently assumes. The September 16, 1948, and November 16, 1948 series, Figures 7 and 8, represent the majority of the cases studied. Different symbols are used for the individual soundings of a series. Location of each sounding area is given on the inserted map, which also indicates the average wind direction. The graphs show the usual slight decrease in potential temperature throughout the ground layer, and the increase through the inversion. The mixing ratio gradient changes from a small negative value in

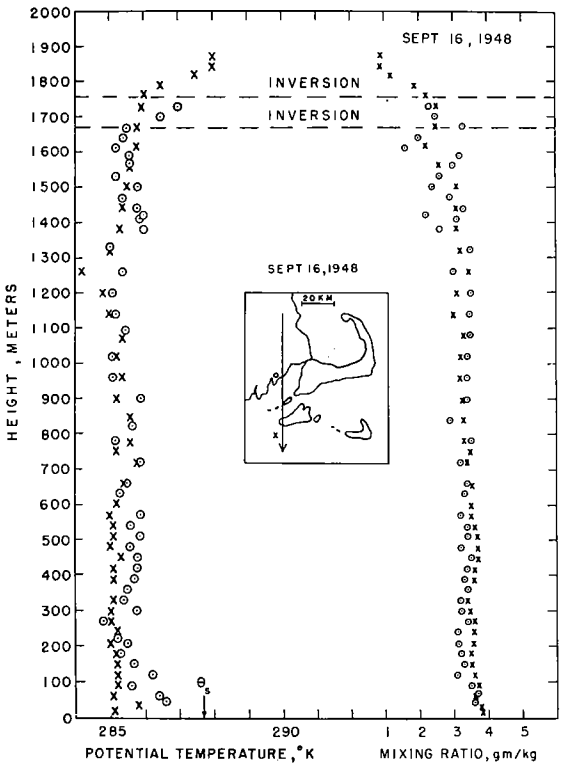

FIG. 7. Potential temperatures and mixing ratios of the ground layer observed September 16, 1948, plotted against height. Symbols apply to sounding indicated in map insert. Dashed lines denote the base of the inversion.

the lower regions to a large negative value in the inversion region. The increase of both the mixing ratio and the mixing ratio gradient during the passage of the air over the water is evident. The θ_s entered on the temperature scale is the sea water temperature reduced to 1000 mb as though it were an air temperature.

The case of September 1, 1948, Figure 9, is discussed here to demonstrate the effect of the

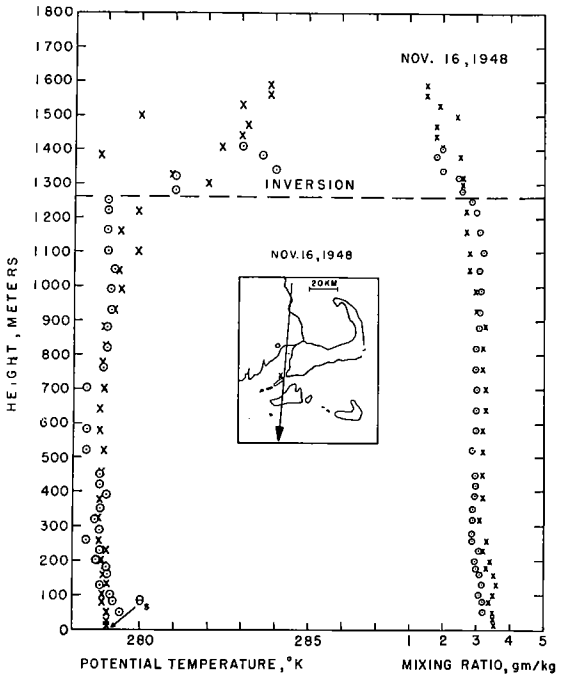

FIG. 8. Potential temperatures and mixing ratios of the ground layer observed November 16, 1948, plotted against height. Symbols apply to sounding indicated in map insert. Dashed lines denote the base of the inversion.

cessation of auto-convective currents on the transport of water vapor, and on the coefficient of turbulent mass exchange. Instability conditions occurred over the heated land on this day, which caused active convection. As the air blew out over the water, first neutral, and then slight stability was established, since the air and water were of about the same temperature. Without the heating from below no new currents could be generated, but the parcels already heated by the land continued to rise until they reached the temperature inversion. The visible manifestation of the termination of convective currents was the presence of 2/10 sky coverage of cumulus clouds over the land, and the absence of cumulus beyond a distance of 12 km offshore.

The transport of water vapor through the 200 m surface, presented in Table III, decreased by a factor of nearly twenty between the first 12 km of the air's measured trajectory over the

water and the remaining 20 km. As this division separates the region of auto-convection from the region of purely turbulent transport, most of the decrease in transport is attributed to the cessation of auto-convection. The change in turbulence

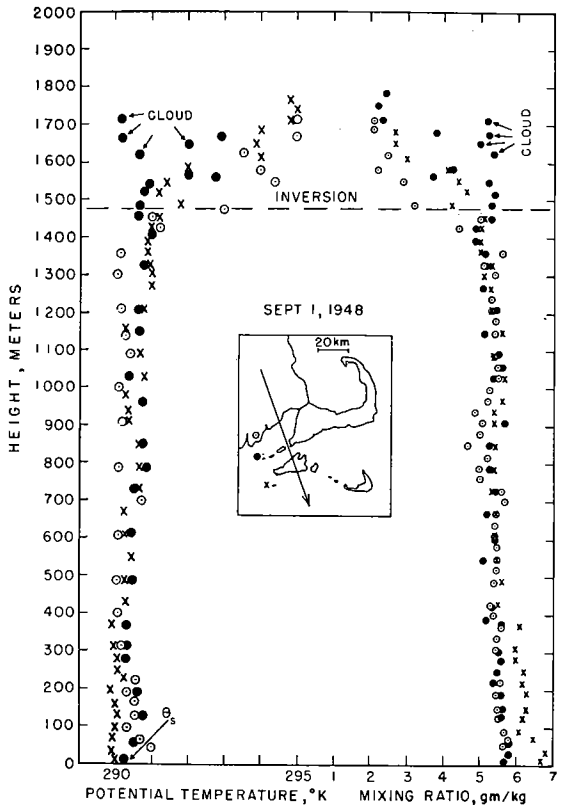

FIG. 9. Potential temperatures and mixing ratios of the ground layer observed September 1, 1948, plotted against height. Labelled points were observed in clouds.

associated with the change from a condition of instability to one of slight stability also contributed to the decrease.

As the moisture gradients became steeper with offshore distance, while the transport decreased, a tremendous decrease in the exchange coefficient is indicated. It is seen from Table VI that the coefficient did decrease from the high value of 15,000 gm cm^{-1} sec^{-1} to the low value of 340 gm cm^{-1} sec^{-1}. Further discussion of this decrease will be made in Section IV.

The data of the last sample presented were obtained on February 3, 1950, over the Gulf of Maine. Only two soundings were made, one over Portland and one over the water. In Figure 10 the observed dry-bulb and dew-point temperatures are plotted on a pseudo-adiabatic diagram to show the modification of the air as it moves over 130 km of water. Noteworthy are the large downwind increase in the frost-point temperatures, and the exceedingly strong inversion. Figure 3 shows the haze layer associated with this inversion. The turbulence index (see sub-section 8 for definition) of the overland sounding is plotted to the left of the temperatures. The plot shows the sudden damping of the ground layer turbulence by the inversion. On the surface weather map the flight path of the plane and the positions of the two soundings have been drawn.

5. *Stabilities of the air column and heights of the ground layer inversion.*

Several quantities have been determined from the data of each sounding which have proven to be helpful in the study of transport and turbulence. Use of these values will be made in later discussions. The stability, defined as

$$\frac{\left(\frac{\partial T}{\partial z} + \Gamma\right)}{T}$$

has been computed for two thicknesses of the column. One value includes both the bottom and upper regions of the ground layer, while the other represents the stability condition of the inversion region. The stability of the inversion region cannot be measured precisely, as the upper boundary is somewhat indeterminate, and frequently was not reached by the sounding aircraft.

The height of the base of the inversion has been read from plots of the temperature and mixing ratio against height. In most cases the base of the inversion can be determined within a few tens of meters from either the mixing ratio or the potential temperature. In a few cases the base is more diffuse and can be determined only within fifty or a hundred meters.

Table II contains these values, together with the mixing ratio gradients and other information concerning the date and relative positions of the soundings. The method of determining the gradients of the mixing ratio is described in Section III, 7.

6. *Water vapor flux and evaporation.*

a. Computation.

Consider an air column flowing from land out over water with its top surface defined by an

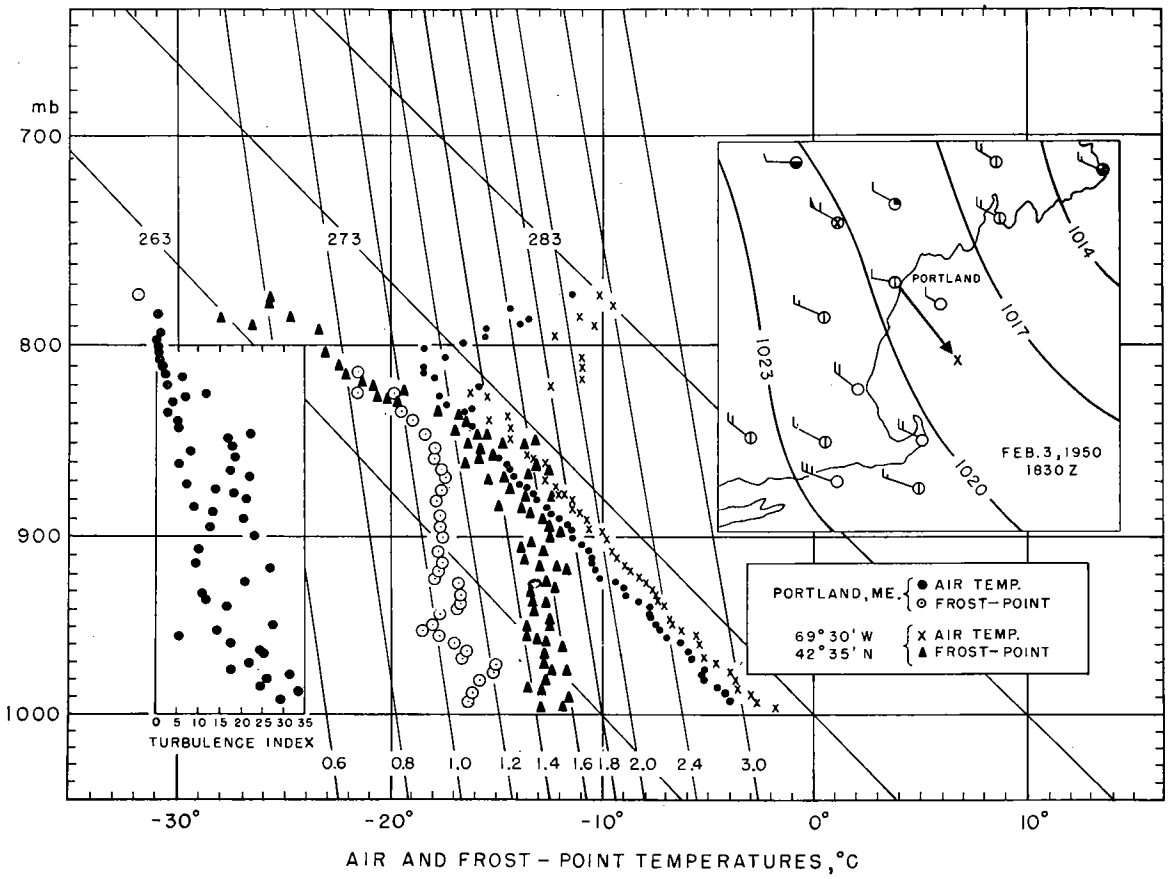

FIG. 10. Dry-bulb and dew-point temperatures of the ground layer observed February 3, 1950, plotted on a pseudo-adiabatic diagram. Simplified surface weather map shows location of soundings and winds. Insert on left gives the turbulence index values observed over land.

inversion region which may vary in height. The horizontal area of the column will expand or contract as the atmosphere subsides or ascents. The continuity equation describing the diffusion of water vapor through any horizontal surface within the column is:

$$A\frac{\partial q}{\partial z}\Big)_{z_1} = \rho\int_{z_1}^{H}\left(w\frac{\partial q}{\partial z}+u\frac{\partial q}{\partial x}\right)dz \qquad (4)$$

where large-scale averages are considered. It is assumed that a steady state exists initially at the shore line and at any fixed point downwind. A represents the average coefficient of turbulent mass exchange at the height z, and may include effects of convection as will be discussed later. u represents the average horizontal wind, w the average vertical wind component, ρ the density of the air, q the mixing ratio, and H the height of the inversion region at which it is assumed that the flux is zero. If $w = 0$, $H_{x1} = H_{x2}$, then

$$A\frac{\partial q}{\partial z}\Big)_{z_1} = \rho\int_{z_1}^{H} u\frac{\partial q}{\partial x}dz \qquad (5)$$

This form of equation (4) has been used in determining the flux as little or no large scale subsidence occurred. Equation (5) has been evaluated by the following summation, which is its equivalent.

$$A\frac{\partial q}{\partial z}\Big)_{z} = \frac{\bar{u}}{g(x_2-x_1)}\left(\sum_{P_z}^{P_H} q_2\,\Delta p - \sum_{P_z}^{P_H} q_1\,\Delta p\right) \qquad (6)$$

Here increments of pressure are used in place of height increments. The average wind has been used and is discussed later. The values of the mixing ratio are taken directly from the soundings made at x_1 and x_2. An additive term has been applied to the resulting fluxes determined from equation (6) in the cases of a few series of observations which are studied in greater detail. This term represents the flow of water vapor through the inversion, which was considered equal to zero

TABLE II

HEIGHT OF THE GROUND LAYER INVERSION STABILITIES, AND MIXING RATIO GRADIENTS

Series Number	Date	Sounding Number	Offshore Distance km	Height of Ground Layer Inversion m	Stability of Ground Layer $cm^{-1} \times 10^{-8}$	Stability of Inversion Region $cm^{-1} \times 10^{-8}$	Mixing Ratio Gradient Bottom Region $cm^{-1} \times 10^{-9}$	Mixing Ratio Gradient Upper Region $cm^{-1} \times 10^{-9}$
1	9/1/48	#1	0	1365	0.0	2200	−15	−2.9
		#2	12	1550	0.2	2000	−12	−2.6
		#3	32	1550	2.1	1500	−60	−11.0
2	9/15/48	#1	0	1865	0.6	640	−14	−1.0
		#2	12	1815	1.7	....	−23	−9.0
		#3	32	1815	2.3	240	−39	−10.0
3	9/16/48	#1	0	1670	0.2	380	−29	−2.3
		#2	43	1555	0.8	720	−11	−5.5
4	9/22/48	#1	0	730	0.8	800	−7.0	−2.8
		#2	12	520	0.7	460	−14	−8.2
		#3	32	550	0.0	1600	−4.0	−4.8
5	9/23/47	#1	0	1300	0.7	670	−5.0	−1.0
		#2	3	1090	0.7	660	−7.5	−12.0
		#3	8	1060	0.7	450	−13	−5.5
		#4	16	1000	0.7	550	−20	−5.5
6	10/1/47	#1	0	1035	0.2	550	−32	−12.0
		#2	3	1065	−0.2	450	−10	−10.0
		#3	8	1035	0.2	370	−7	−8.0
		#4	16	1245	−0.6	460	−12	−7.0
7	10/20/49	#1	180	315	3.0	1200	−24	−24.0
		#2	280	315	3.0	1200	−14	−14.0
8	11/9/47	#1	0	....	0.2	....	−5.2	−.01
		#2	16	....	−0.4	....	−12	−4.4
9	11/10/47	#1	0	1065	0.0	640	−1.5	+0.9
		#2	8	1065	0.0	450	−8.6	−4.3
10	11/13/47	#1	0	....	0.2	....	−3.0	−2.0
		#2	8	....	0.0	210	−3.3	−3.3
11	11/16/48	#1	0	1250	−2.0	1600	−13.0	+2.2
		#2	24	1220	0.7	710	−10	−5.7
12	11/17/47	#1	0	1180	−7.4	930	+1.2	−1.8
		#2	3	1180	−7.0	1000	−9.9	−2.4
		#3	10	1120	−4.6	2100	−23	−3.5
		#4	17	1150	−4.4	830	−9.1	−5.5
13	12/30/49	#1	0	450	0.8	710	−0.5	−0.5
		#2	10	565	0.8	620	−8.3	−3.6
		#3	120	1010	1.3	640	0.0	+1.0
14	1/17/50	#1	0	1225	−1.8	510	−3.0	−1.4
		#2	20	....	0.0	....	−6.6	−2.3
		#3	150	1140	−0.4	770	−1.0	−0.4
15	2/3/50	#1	0	1550	0.0	1300	−1.0	−1.0
		#2	130	1550	0.7	1500	+0.5	+0.5

in developing equation (6). The value of the additive term is about two orders of magnitude smaller than the value of the flow through the bottom of the ground layer. It is based on the study mentioned in I.

The phenomenon of local subsidence of an air mass leeward of a shore line was not anticipated at the beginning of the observational program, and, when first noted, caused doubt concerning the validity of the mixing ratio measurements. It was noticed that the air column 3 km offshore was frequently drier than it had been over the land, in spite of its passage over warmer water. A cross-section diagram drawn from the October 1, 1947 data (Figure 11) shows that first a drying of the air occurs, and then a rapid increase in the moisture content of the air, as diffusion becomes predominant. The dip in moisture isograms may be explained as the result of subsidence a few kilometers offshore.

While no direct measurement of subsidence was made on this day, observations of the surface wind velocity show that the velocity increased downwind over the water by about 2 m/sec. If the winds aloft remained the same or decreased, then continuity of mass demands that the air subside over the water.

A check was made of U. S. Weather Bureau pilot balloon records on hand at the Institution to see if any pattern leading to subsidence was formed during days with strong offshore winds. It was found that the winds in the lower levels over Nantucket Island (50 km offshore) were frequently greater than at Boston, Massachusetts, or Portland, Maine. Also it was noted that the Nantucket winds at higher levels (above 1000 to

1500 m) were lower than the Boston or Portland winds.

Another cross-section which indicates a limited region of subsidence near the leeward shore has been constructed from the September 22, 1948

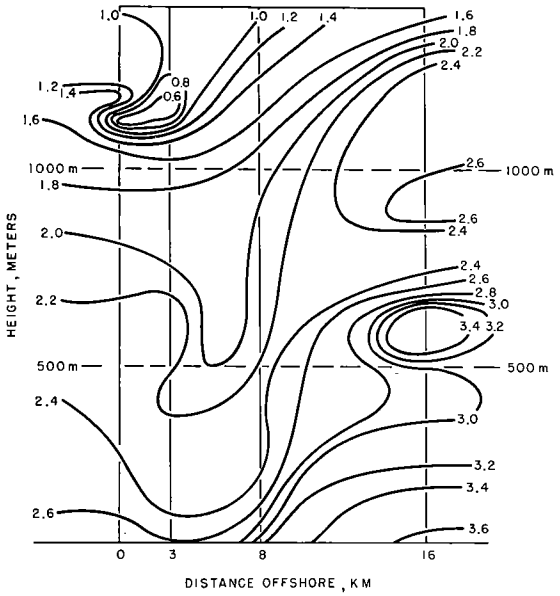

FIG. 11. Mixing ratio isograms observed October 1, 1947, exhibit a depression 3 km offshore caused by local subsidence.

data (Figure 12). In this case, also, the moisture isograms slope sharply downward at the shore line, and then slowly ascend downwind.

The only direct evidence of subsidence was found by a sounding airplane equipped with an accelerometer making horizontal runs perpendicular to the leeward shore of Nantucket Island. The records, made in connection with the study of air flow over a heated island, show downdrafts 1–3 km offshore capable of producing downward accelerations of the airplane of about 400 cm sec^{-2}. Downdrafts of this magnitude are much larger than turbulence alone could produce under the same wind and stability conditions. Malkus and Stern of this Institution, in their as yet unpublished theoretical study of flow over the heated island, find that subsidence occurs at the leeward shore of an island under a wide range of heating, turbulence, stability, and wind velocity conditions.

The effects of local subsidence on the determined value of water vapor flux could not be evaluated and used in equation (4). Errors due to its occurrence are minimized by averaging the moisture content in the air columns over the land and 3 km downwind over the water, and using the average as a measure of the original undisturbed air mass. The average downwind distance was adopted as the zero point for the flux determination.

Larger height variations of the ground layer arise from two sources, (1) the vertical stretching or shrinking of the air of the layer due to convergence or divergence, and (2) the inclusion of the inversion air into the ground layer or the exclusion of air from the ground layer. The inclusion or exclusion of air is accomplished through the process of destroying the original inversion and of forming a new inversion at a higher or lower level. The first source may be accounted for by equation (4).

Many variations observed have been attributed to the second process which is capable of causing

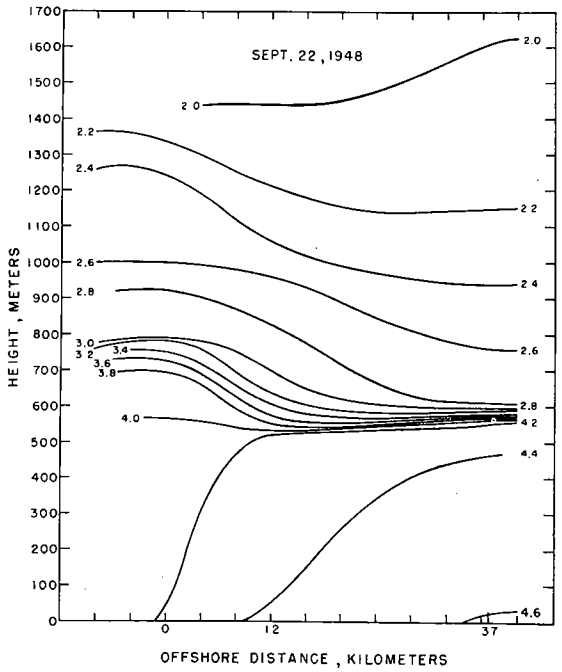

FIG. 12. Vertical cross-section of air constructed from September 22, 1948 data. Mixing ratio isograms indicate change in height of inversion and diffusion of water vapor.

large variations in relatively short distances. The balance of the turbulent energy of the air of the ground layer and the stability of the overlying air determine whether the turbulent air will destroy the existing inversion and build up into the air of

the advection layer, or whether the turbulence will be unable to continue to mix the air in the region of the inversion, causing a lowering of the inversion. These changes have been described by Wood (1937) in detail. To compute the flow, the height adopted for substitution in equation (6) is the final height of the inversions observed in a given series of soundings. With this convention, the smallest error in determining the accumulation of water vapor in the atmosphere is made, and a reliable value of the flow is obtained. In the case of a low final height resulting from causes other than subsidence, the measured accumulation may be systematically low by a small (0–5%) amount.

The pilot balloon data, both U. S. Weather Bureau and local, were used for the flow computation. The wind speed and direction averaged over the entire ground layer was considered best for this work. In the case of stable air masses the turbulence is weak so that the air aloft moves faster than, and does not mix rapidly with, the lower air, thus causing the phenomenon of shearing stratification, as described by Craig (1946). In less pronounced cases of stability, and in neutral and unstable air masses, this stratification cannot develop because of the rapid mixing of the air. The characteristic frictional shearing of the wind with height is present, but this does not imply that a particular parcel of air travels long distances at one height. Rather, through the mixing process of eddy diffusion, it will be dispersed throughout the ground layer. For this reason it is correct to use the mean value of the velocities of the air at different heights to determine the trajectories of the air. In the reduction of these observations and the computation of flux and austausch values, this principle is used in cases where there is evidence of sufficient mixing. This allows treatment of the ground layer as a single body moving with a given velocity.

The flux of water vapor has been found for two surfaces, one at the surface of the water, synonymous with evaporation, and another 200 m higher. The values found are presented in Table III. The units are gm cm^{-2} sec^{-1} x 10^{-6}.

In the following section the variation of the coefficient of turbulent mass exchange with height is computed. These computations are based on the following smooth average values of the flow of water vapor through surfaces at various heights.

TABLE III

EVAPORATION AND WATER VAPOR FLUX

Series Number	Date	Offshore Distance km	Evaporation at Surface gm cm^{-2} sec^{-1} x 10^{-6}	Flux at 200 m gm cm^{-2} sec^{-1} x 10^{-6}
1	9/ 1/48	0–12	44.0	43.0
		12–32	9.3	2.3
		0–32	22.0	14.0
2	9/15/48	0–12	14.0	4.2
		0–32	10.0	3.2
3	9/16/48	0–43	3.7	1.7
4	9/22/48	0–12	6.1	4.2
		0–37	4.9	3.9
		12–37	4.1	3.7
5	9/23/47	1–14	7.3	4.9
6	10/ 1/47	1–8	24.0	17.0
		8–16	91.0	40.0
		0–16	58.0	28.0
7	10/20/49	180–280	2.6	1.3
8	11/ 9/47	0–16	19.0	13.0
9	11/10/47	0–8	28.0	14.0
10	11/13/47	0–12	28.0	24.0
11	11/16/48	0–24	3.8	1.4
12	11/17/47	0–3	12.8	8.2
		3–10	7.2	0.9
		10–17	11.0	6.9
		0–17	10.2	5.1
13	12/30/49	0–10	16.0	9.0
		10–120	8.3	7.1
14	1/17/50	0–20	8.3	7.4
		20–150	4.0	3.6
15	2/ 3/50	0–130	7.8	7.2

The values presented in Table IV are the averages of four soundings, selected for their freedom from the influences of changing height of inversion, uncertain or low inversion height, pronounced convective activity, or increasing stability. An arbitrary flow of 10 x 10^{-7} gm cm^{-2} sec^{-1} through the base of the inversion has been added to the average values in accordance with the maximum value previously found and described. The averages were plotted against height and smoothed values obtained from a mean curve. Smoothed and unsmoothed values are entered in Table IV. Heights are expressed in terms of percentages of the height of the base of the inversion.

TABLE IV

WATER VAPOR FLOW THROUGH SURFACES AT PARTICULAR HEIGHTS

Height % of Inversion Height	Unsmoothed Flow gm cm^{-2} sec^{-1} x 10^{-7}	Smoothed Flow gm cm^{-2} sec^{-1} x 10^{-7}
0	135	135
10	—	108
20	85	85
40	54	52
60	29	30
80	12	16
100	10	10
110	—	8

b. Empirical flux relations.

An attempt has been made to relate the water vapor flux to the meteorological elements of the

air mass and water surface prior to the passage of the air over water. Many elements, including wind speed, height of ground layer, difference in mixing ratio between the unmodified air and the saturation mixing ratio in the laminar sub-layer in contact with the water surface, stability of the air column, and angle between the surface wind and the gradient wind, have been examined for any subsequent influence on the flux. Most of these elements, when plotted against flux, exhibited a great scatter of the plotted points, indicating that the flux is not determined exactly by any one of the basic meteorological parameters. The greatest success was obtained by plotting

$$(w_s - \overline{w}_1)\left(\frac{\overline{W}}{10^8|S| + 1}\right)$$

against the 200 m flux, Figure 13. Here w_s is the saturation mixing ratio existing in the air actually

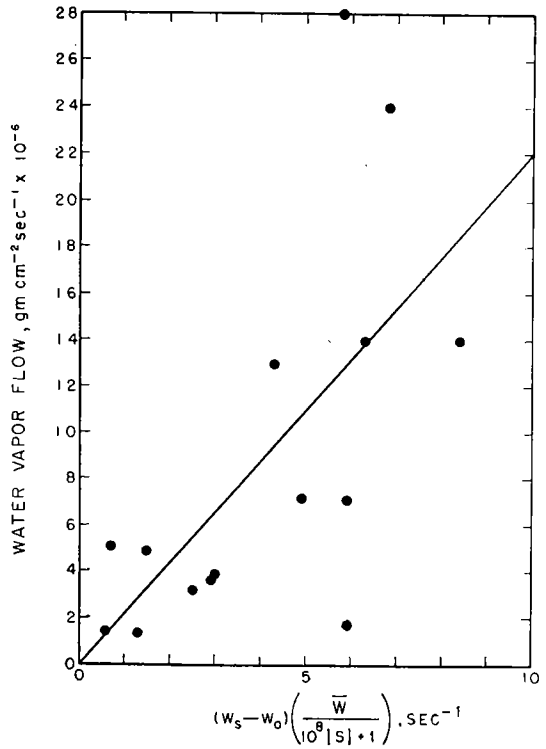

FIG. 13. An empirical water vapor transport relation. Water vapor flux has been plotted against the quotient of the mixing ratio difference times the wind speed, divided by 10^8 times the stability plus one.

in contact with the water, $\overline{w}_1$, the original average mixing ratio in the ground layer up to the inversion region, $\overline{W}$, the average wind speed of the ground layer, and $|S|$, the absolute value of the stability of the air column. Even this comparison shows considerable indeterminancy. The combination of parameters was tested when it was noted (see the following sub-section 7, Figure 19) that a relation existed between $(w_s - \overline{w}_1)$ and the subsequently established $\frac{\partial q}{\partial z}$. Similarly, the $\frac{\overline{W}}{10^8|S| + 1}$ factor was found in Section IV, 1, Figure 24, to be a measure of the coefficient of turbulent mass exchange. The product of these two factors then represents the $-A\frac{\partial q}{\partial z}$ term of the diffusion equation, and should equal the water vapor flow.

7. *Vertical gradients of the mixing ratio.*

The sounding procedure described in Section II was adopted to make certain that any gradients determined would not be affected significantly by the thermal lag of the sensing elements. The final lag of the temperature elements behind the environment upon arriving at a given level can be shown to be negligibly small. With a rate of climb of 200 feet per minute, a dry-bulb lag coefficient of 4 sec., a dry-bulb lapse rate of 9 C per 1000 m, a wet-bulb lapse rate of 6 C per 1000 m, and assuming that the wet-bulb lag is the same rather than less than the dry-bulb lag, then the dry-bulb temperature will lag behind its environment by 0.036 C while the wet-bulb lags by 0.024 C. These values are, of course, negligibly small in the determination of the mixing ratio, and the mixing ratio gradients can be considered accurate within the limits stated in Section III, 2.

The mixing ratio gradients have been determined graphically, although a few were computed by the means of least squares. The values, presented in Table II, have been determined by fitting straight lines to the observations of each sounding. One line was fitted to the observations in the 20 to 200 m region. The slope of this line is considered to represent the gradient in the bottom frictional region. The fitting of the observations into a linear form in this region is not intended to contradict the well-established logarithmic relation found by other investigators (see Berry, Bollay and Beers, 1945) in the lowest 30 to 40 m above the surface. Figure 14 is a composite mixing ratio curve of the bottom region made by averaging adjusted observations of six soundings made 16 to 24 km offshore. The straight line corresponding to a gradient of

-11×10^{-9} cm^{-1} appears to be a satisfactory fit of the observations. Since only two observations were made below 40 m, it was not attempted to establish a logarithmic relation.

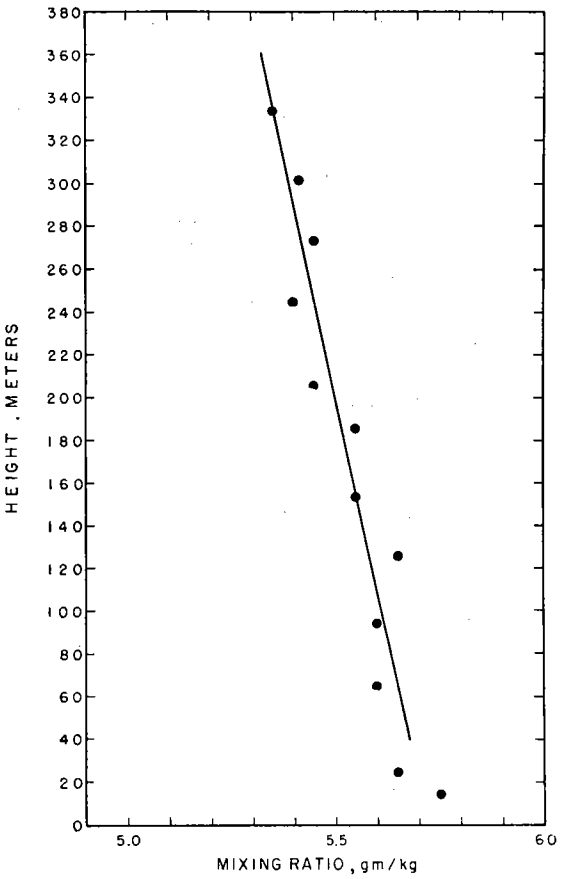

FIG. 14. Composite mixing ratio-height curve of the bottom region of frictional influence. Average of six soundings.

Other composite curves have been constructed in the following manner. All heights were expressed as percentages of the inversion height at the time of observation. Averages of the mixing ratios for each 5% height range were computed for each sounding. The average value computed for each height range from the individual sounding averages has been plotted in Figures 15, 16 and 17 to form composite mixing ratio curves for three offshore distances: (1), 12–24 km; (2), 32–43 km: and (3), 120–150 km.

The set of data for the 12–24 km offshore distance has been smoothed by reading values from a mean curve through the average points. The smoothed data for the curve fitting are tabulated below, in Table V.

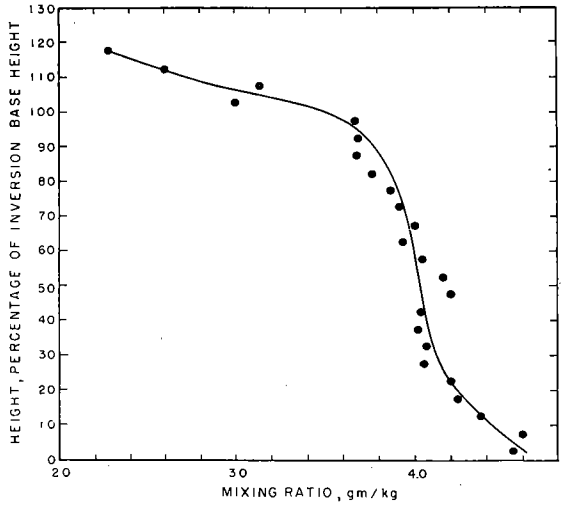

FIG. 15. Composite mixing ratio-height curve of ground layer, 12–24 km offshore. Average of six soundings.

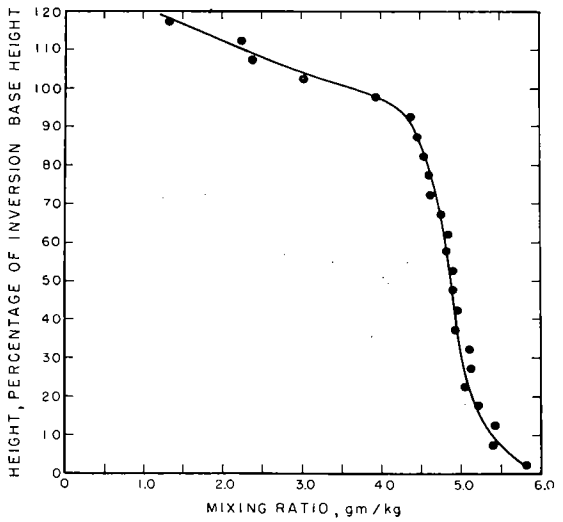

FIG. 16. Composite mixing ratio-height curve of ground layer, 32–43 km offshore. Average of four soundings.

TABLE V

SMOOTHED DATA FOR MIXING RATIO CURVE FITTING TESTS
AVERAGES OF SOUNDING 12–24 KM OFFSHORE

Height % of Inversion Height	Mixing Ratio gm/kg	Height % of Inversion Height	Mixing Ratio gm/kg
0	10.40	60	4.00
5	4.56	70	3.96
10	4.43	80	3.90
20	4.24	90	3.78
30	4.12	100	3.50
40	4.07	110	2.72
50	4.03		

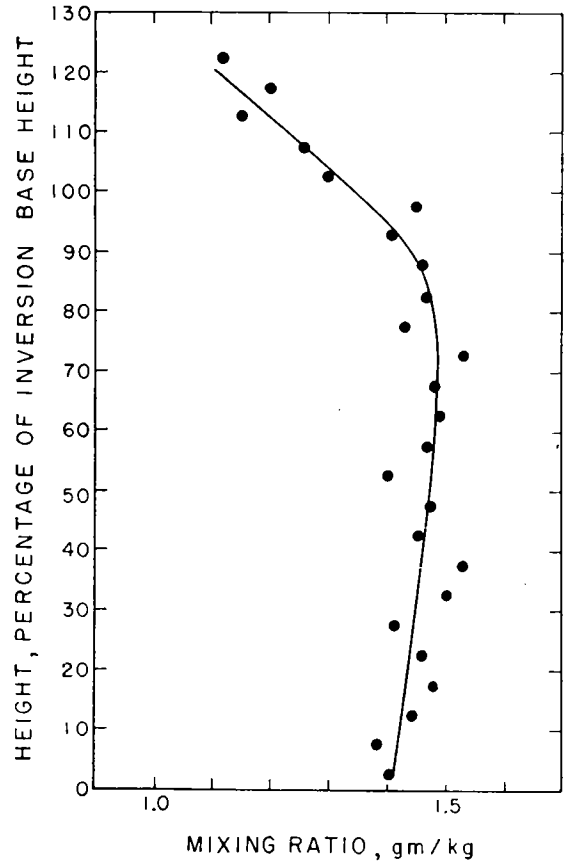

FIG. 17. Composite mixing ratio-height curve of ground layer, 120–150 km offshore. Average of three soundings.

In Section IV, 2, it is shown that, if E, the flow through a surface, and A, the eddy diffusion, are both constant, then

$$q_z = q_a - (E_a/A_a)\,(z)\Big]_a^z \qquad (7)$$

If E and A are linear functions of z, then

$$q_z = q_a - \frac{\lambda z}{\gamma} + \frac{\gamma E_a - \lambda A_a}{\gamma^2} \log (A_a + \gamma z - \gamma a)\Big]_a^z \qquad (8)$$

If E is constant, but A is linear, then

$$q_z = q_a - \frac{E_a}{\gamma} \log (A_a + \gamma z - \gamma a)\Big]_a^z \qquad (9)$$

If E is linear, but A is constant, then

$$q_z = q_a - \frac{E_a}{A_a}(z) + \frac{\lambda}{2A_a}(z^2)\Big]_a^z \qquad (10)$$

If the various combinations of variations of E and A obtain in different regions of the atmosphere, then the mixing ratio curve will necessarily be a combination of the functional forms mentioned above. A pertinent point to be investigated is whether the mixing ratio curves in any regions of the ground layer present functional forms corresponding to the four stated above.

By plotting the values of the mixing ratio against a linear height scale, Figure 15, it is seen that small segments of the resulting curve can be represented by a straight line, but the whole curve cannot. However, since we know from both theory and observation that the constancy of E and A holds only in limited regions, the fit of simple linear functions to parts of the curve cannot be accepted as a significant description of the variation of the mixing ratio in the ground layer.

Trying the logarithmic function, equation (9), we plot mixing ratio values against the logarithm of the height (Figure 18). When this is done it is

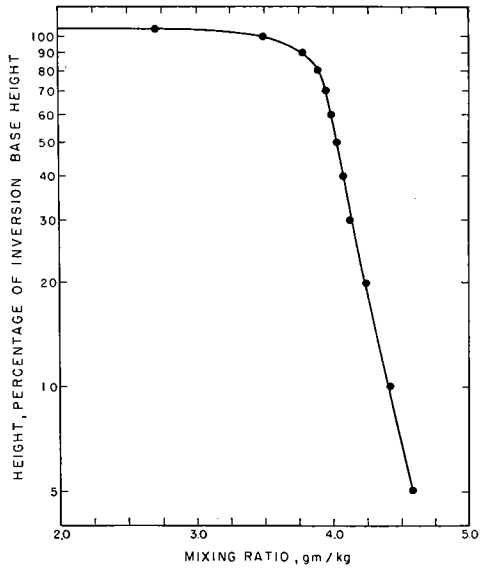

FIG. 18. Mixing ratio values plotted against the logarithm of the height.

apparent that, above the 30% level, the curve departs from a straight line. A second straight line departs from the observations above the 60% level.

The suitability of a function, $q = f(a - bz - cz^2)$, may be tested by noting the constancy of the second differences of q when tabulated as a function of equal increments of z. For

nine steps, the second differences are +.03, −.07, −.01, −.01, +.01, +.02, +.06, +.14, and +.50. The small values between the 40% and 80% levels are well within the observational errors and indicate that the function represents the data throughout well more than 40% of the ground layer.

The suitability of a function, $q = f(a - bz - c \log dz)$, may be demonstrated by plotting values of the mixing ratio against values of $z/1000 + \log z$ (Figure 19). One straight line fits the observa-

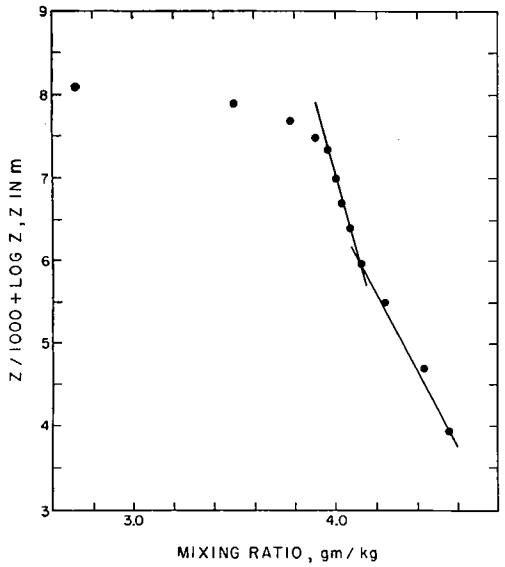

FIG. 19. Mixing ratio values plotted against $z/1000+\log z$.

tions in the 5% to 30% region, while another line fits the observations from the 30% level to the 70% level. It is concluded that $q = f(a - bz - c \log dz)$ describes the mixing ratio curve throughout 75% of the ground layer. This demonstrates that the assumption of the linearity of both E and A in each of two segments of the ground layer is a reasonable one, as will be discussed in a later section.

An empirical relation, already mentioned in the previous sub-section, was found to exist between the mixing ratio gradient over the water and the difference between the saturation mixing ratio over the water surface and the average mixing ratio value of the original air mass. This relation and the scatter of the observed values are shown in Figure 20.

8. *Turbulence index, and gust velocities.*

The accelerometer records obtained during the flights of the Stinson Voyager and the DC-3 have been reduced to a quantity called the *turbulence index*, while data obtained in the Lockheed Electra have been reduced to effective vertical gust velocities. The turbulence index is defined as the area enclosed by a line forming the envelope of the peak accelerations for a fixed time interval. The defining area has been drafted on an accelerometer trace in Figure 21. The areas have been measured with a polar planimeter. One turbulence index unit equals an area of 0.01 sq. in. on the record, has the dimensions of velocity, and represents the average absolute value of the vertical velocity attained by the airplane due to the turbulence of the air. An atmospheric turbulence capable of producing alternate positive and negative vertical accelerations of the airplane equal to 100 cm sec^{-2} will have a turbulence index of 24.

The significance of the turbulence index lies in the fact that its value is determined by the magnitude of vertical currents in the air. It is

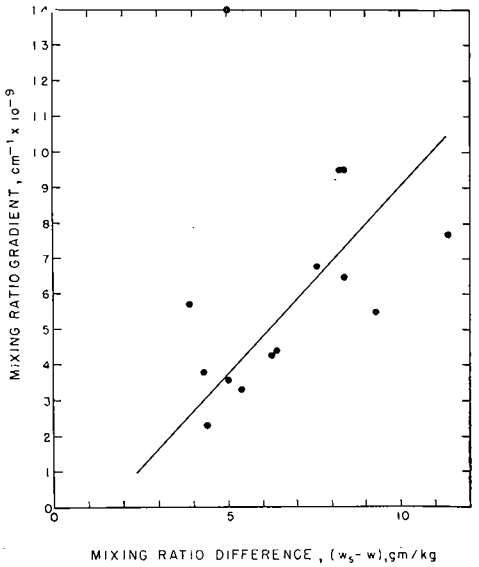

FIG. 20. Empirical relation between the mixing ratio gradient in the upper region of frictional influence over water and the saturation mixing ratio at the water temperature less the original mixing ratio of the air mass.

tacitly assumed in applying the turbulence index to diffusion analysis that the airplane and accelerometer respond to the same gusts that are instrumental in the transport of air parcels. Actually,

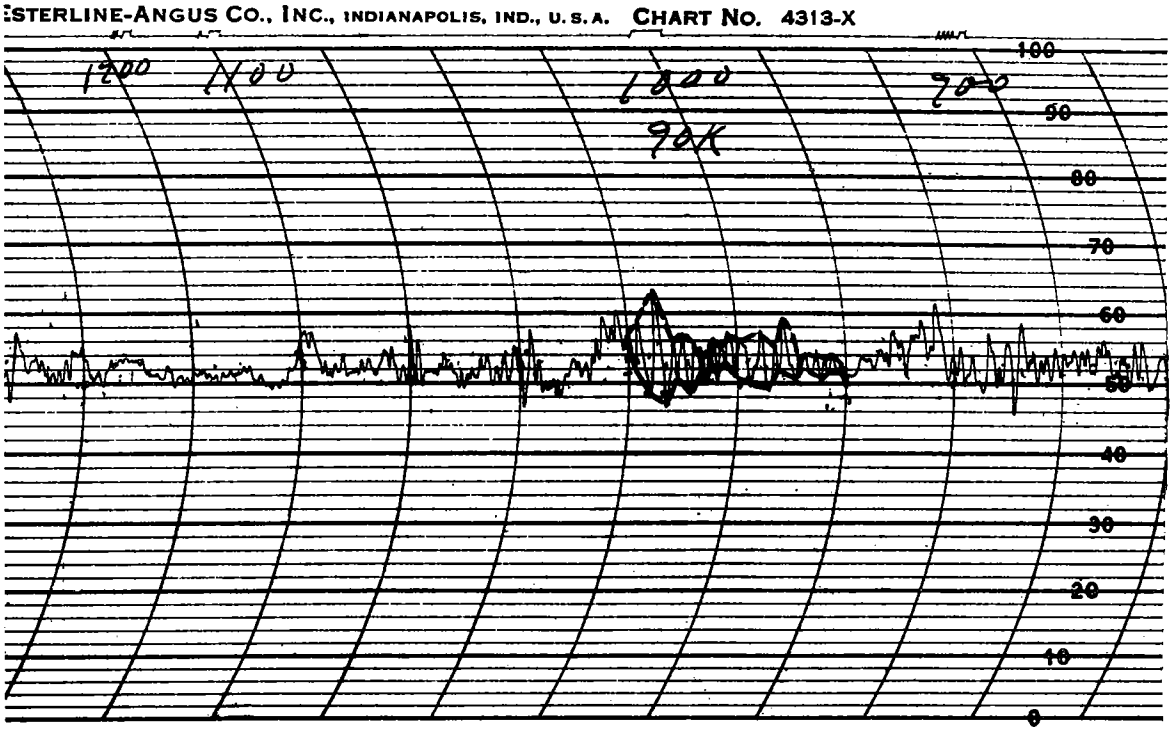

FIG. 21. Accelerometer trace obtained October 20, 1949, with drafted line defining turbulence index.

an airplane is highly selective in its response to gusts of various frequencies, and can only approxi-

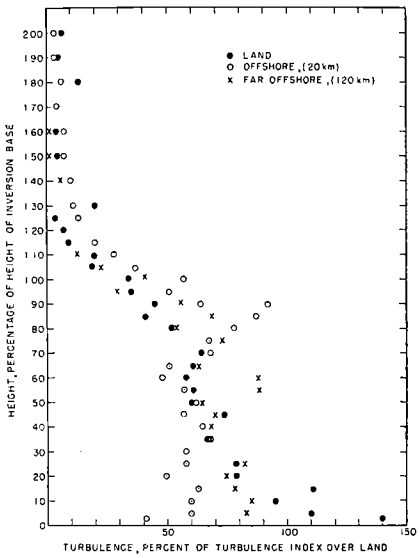

FIG. 22. Turbulence index variation throughout the ground layer observed 20–30 km offshore, and 120–150 km offshore.

mate the response of an air parcel. Further, the turbulence index corresponds to the vertical gustiness, and cannot be identified with the coefficient of turbulent mass exchange, defined as $\rho\ \overline{wl}$ by the mixing length theory. In spite of these limitations on the interpretation of the index, it is of great value since it can describe the vertical gustiness of the atmosphere, and it is so easily observed at all heights and positions in the ground layer.

Changes of the turbulence index throughout the ground layer and with distance offshore are shown in Figure 22. In this diagram heights are expressed as a percentage of the height of inversion base, so that averages may be obtained from observations obtained on several days. In order that averages may be obtained from days with varying degress of turbulence, the turbulence index is expressed as a percentage. The average of the indices for the lowest 300 m over land on a given day was adopted as 100%.

One feature of the ground layer noted on the diagram is the small negative gradient of the turbulence index in the 20% to 80% height range. This means that the magnitude of the gust velocities affecting the airplane are essentially constant throughout the region. When the small change in

gust velocities is considered in conjunction with the more rapid decrease of the coefficient of turbulent mass exchange discussed in Section IV, 2, Figure 25, it becomes apparent that the mixing lengths associated with the gusts change with height.

The suppression of turbulence by the inversion is demonstrated by Figure 22 which shows the exceedingly rapid decay of turbulence through the inversion. The transition from the turbulent air to the smooth air of the inversion is more pronounced in individual cases than the average values indicate. The difference arises from the existence of gusts that break through the sharp interface. Many individual accelerometer traces have recorded intense gusts in the vicinity of the inversion. These may be associated both with the strong wind shear existing through the inversion and with the occasional convective currents present in the ground layer.

In the lowest 10% height range a sequence of changes in the turbulence is produced by the passage of the air over the water. Over the rough tree and house-covered land the turbulence was intense, causing a rapid succession of short-lived accelerations of the plane up to 500 cm sec^{-2}. A few kilometers offshore the turbulence had moderated to only a small fraction of the original intensity. Further offshore (135 km) the turbulence increased again but did not attain its original value.

In contrast to the large turbulence variations in the lowest levels, the turbulence in the main body of the layer does not change more than a few percent. The greatest modification appears in the gradient, which is negative over land, slightly positive over the offshore region, and negative again over the more distant offshore waters.

Brewer (1949)[2] in an unpublished report calibrated the response of the Lockheed Electra airplane to the vertical gustiness of the air in such a manner that the effective vertical gust velocities can be determined directly from the accelerometer records. The calibration is based on the assumptions of sharp fronted gusts, rigid wings, and other simplifications of the aerodynamic properties of

[2] G. A. Brewer. A procedure for determining the approximate velocities of gusts encountered by sounding aircraft. Unpublished report No. 044 on file at Woods Hole Oceanographic Institution.

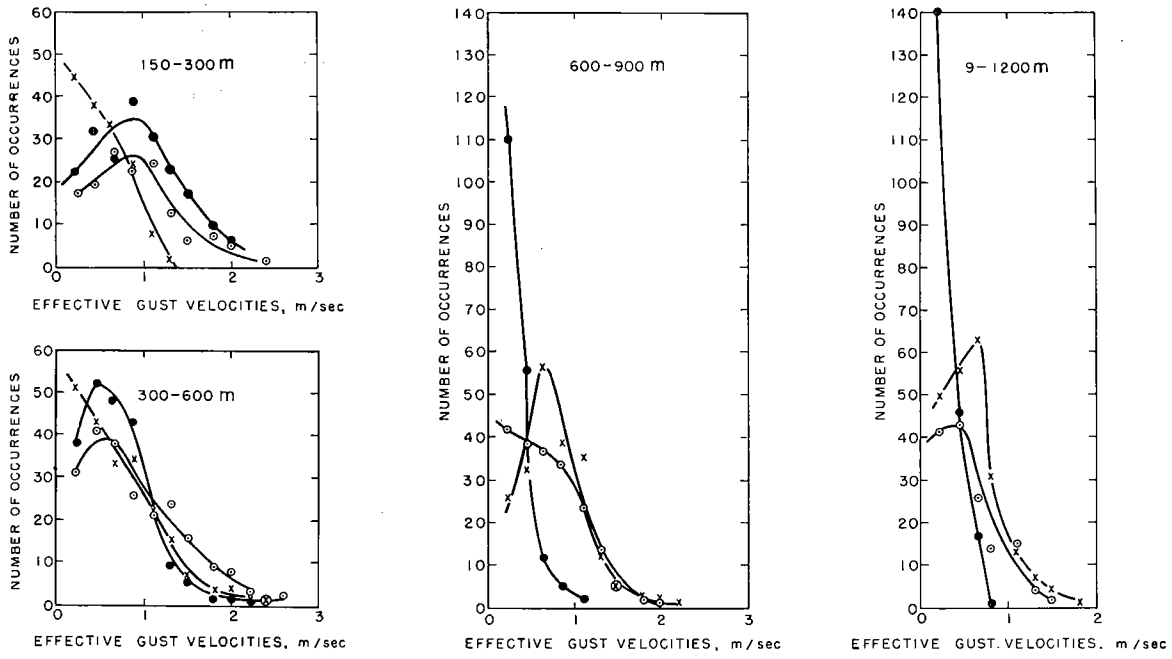

FIG. 23. Effective gust velocities occurring December 30, 1949, in four height ranges over land, 10 km offshore, and 120 km offshore.

the airplane. The true gust velocity cannot be calculated exactly, but is of the order of 40–60% larger than the effective gust velocity (Rhode, 1937). With the Electra, a turbulence index of 24 corresponds to an average true vertical gust velocity of 80 cm/sec.

Only the December 30, 1949, and January 17, 1950, series of soundings were made with the Electra, and thus can be treated in the above manner.

The frequency of occurrence of effective gust velocities observed on December 30, 1949, have been plotted for five height ranges, 150 to 300 m, 200–600 m, 600–900 m, 900–1200 m, and 1200–1500 m, in Figure 23. The abscissa is the number of gusts of a particular magnitude that the sounding aircraft encountered in climbing through the designated height range. The data obtained from each of the three soundings, one over land, another 10 km downwind over the water, and the last 120 km downwind over the water, are plotted with different symbols to show the changes that occur in gust magnitudes and frequency distributions.

IV. ANALYSIS OF TRANSPORT IN TERMS OF TURBULENT DIFFUSION AND CONVECTION

1. *Determination of the coefficient of turbulent mass exchange.*

If the net flow of water vapor upward through the ground layer is accomplished by the random turbulent motions of the air and the geometric distribution of the vapor is known, then their values can be substituted in the diffusion equation and the coefficient of turbulent mass exchange determined. In this sub-section, transport will be analyzed without regard for the possibility of free-convective processes contributing to the transport of water vapor. Sub-section 3 will treat this consideration in detail.

To evaluate the exchange coefficient from equation (1) a routine system of determination of gradients and corresponding flux surfaces was adopted. Two gradients were determined from the slope of straight lines determined graphically, one for the region from 20 m to 200 m, the other from 200 m to the top of the layer. The surface flux was matched with the gradient for the lower level. The equation then yields a value repre-

TABLE VI

COEFFICIENT OF TURBULENT MASS EXCHANGE

Series Number	Date	Distance Offshore km	Average $\partial q/\partial z$ Bottom Region $cm^{-1} \times 10^{-9}$	Average $\partial q/\partial z$ Upper Region $cm^{-1} \times 10^{-9}$	Coefficient Bottom Region gm cm^{-1} sec^{-1}	Coefficient Upper Region gm cm^{-1} sec^{-1}
1	9/1/48	0–12	−14	−2.8	3,100	15,000
		12–32	−36	−6.8	260	340
		0–32	−29	−5.5	760	2,500
2	9/15/48	0–12	−19	−5.0	740	840
		0–32	−25	−7.0	400	460
3	9/16/48	0–43	−20	−3.9	190	440
4	9/22/48	0–12	−11	−5.5	560	760
		12–37	−9	−6.5	460	570
5	9/23/47	1–14	−11	−6.0	660	820
6	10/1/47	1–8	−16	−10	1,500	1,700
		8–16	−10	−7.5	9,100	5,350
8	10/20/49	180–280	−19	−19	140	68
9	11/9/47	0–16	−8.6	−2.2	2,200	5,900
10	11/10/47	0–8	−5.0	−1.7	5,600	8,200
11	11/13/47	0–12	−3.2	−2.7	8,800	8,900
12	11/16/48	0–24	−12	−1.8	320	780
13	11/17/47	0–3	−4.4	−2.1	2,900	3,900
		3–10	−17	−3.0	420	300
		10–17	−16	−4.5	690	1,500
14	12/30/49	0–10	−4.4	−2.1	3,600	4,300
		10–120	−4.2	−1.3	2,000	
15	1/17/47	0–20	−4.8	−1.9	1,700	3,900
		20–150	−3.8	−1.4	1,100	2,600
16	2/3/50	0–130	−0.3	−0.3		

sentative of the bottom frictional region, but not associated with any exact height. Likewise, the flux through the 200 m surface, was matched with the gradient for the upper frictional region of the ground layer.

Table VI presents the exchange coefficients expressed in gm cm^{-1} sec^{-1}, corresponding to the distance offshore tabulated in column 3. The average gradients substituted in the diffusion equation are listed in columns 4 and 5. Column 6 represents the values determined for the bottom frictional region, while column 7 represents the values characteristic of the upper frictional region.

One important feature of the turbulence study brought out by the table is the large magnitude of the values of the coefficient of turbulent mass exchange. Prior to this report the coefficient was measured under more stable conditions and values between 1 and 1000 gm cm^{-1} sec^{-1} were thought representative of most conditions encountered in the atmosphere. The present work shows that the exchange coefficient can attain values over such a wide range as 780 to 15,000 gm cm^{-1} sec^{-1} in the unstable case.

Table VII has been compiled to compare these values with the values obtained by a few other workers in the field, and to show the effect of stability. Values of the exchange coefficient determined from heat and momentum transport are also included in Table VII. The table is divided into three columns, representing the stability conditions existing at the time of the experiment. The heading "very stable" is used to denote the existence of an inversion ($S > 40 \times 10^{-8}$ cm^{-1}). A value of the lapse rate lying between the isothermal and nearly the dry adiabatic lapse rate (0.2×10^{-8} $cm^{-1} < S < 40 \times 10^{-8}$ cm^{-1}) is classified as "slightly stable". By "unstable" it is meant that the lapse rate was either found to be nearly neutral or super-adiabatic ($S \leq 0.2 \times 10^{-8}$ cm^{-1}), or that the water or land surface temperature was higher than the air temperature. The name following a value indicates the author responsible for the determination.

Taylor (1915) computed exchange coefficients from studies of the potential temperatures over the cool waters of the Newfoundland Grand Banks. Lettau (1937) made his observations during two free balloon excursions. The diffusivity values given were computed from dust counts and settling rates, as well as from humidity observations. Craig (1949) determined his values of the exchange coefficient from the records obtained with an airplane equipped with a psychrograph identical to the one employed in the present study. The coefficients are determined in a manner, and with an accuracy comparable to the values determined in the present work, which may be considered as an extension of his work to slightly stable and unstable conditions. Jaw (1937) determined the coefficient for water vapor transport from

TABLE VII

COEFFICIENT OF TURBULENT MASS EXCHANGE OBSERVED IN THE GROUND LAYER
gm cm^{-1} sec^{-1}

Property Considered	Stability Class:	Very Stable $>40 \times 10^{-8}$ cm^{-1}	Slightly Stable 0.2×10^{-8} to 40×10^{-8} cm^{-1}	Neutral or Unstable $<0.2 \times 10^{-8}$ cm^{-1}
Water, Vapor, Heat, or Dust		0.9– 8 (Taylor) 17 (Lettau) 0.2–65 (Craig)	400 (Lettau) 90 (Jaw) 450 (Bunker et al) 100 (Riehl et al) 69–2500 (Bunker)	780–15,000 (Bunker)
Momentum		193–782 (Huss)	347–13,200 (Huss) 125–500 (Mildner) 370 (Riehl et al)	1770–262,000 (Huss)

"Meteor" observations in the trade wind region. Bunker, et al (1949) combined the value of the mean annual evaporation and the average mixing ratio gradient measured from airplane soundings. Riehl, et al (1951) made a similar computation using moisture accumulations and gradients averaged from radiosonde observations.

The momentum exchange coefficient was evaluated by Mildner (1932) from a series of pilot balloon observations. The range in variation shown is the height variation of the coefficient. Huss and Portman (1948, 1949) computed the eddy viscosities from wind observations obtained on a radio tower 50 m above the ground, following the method of Ertel (1930). Riehl, et al (1951) have determined the eddy viscosity, using the

same body of observations as for the moisture exchange coefficient computations.

It is readily apparent that large differences occur between the values determined by the different observers, whether diffusivities or viscosities are considered. Part of this difference may be due to the different manners of observation, definition, and calculation of the exchange coefficient. Much of the difference is caused by the large day to day, and level to level variation of the exchange coefficient. From Huss's paper and the present work it is clear that both the diffusivity and the viscosity can vary over wide limits, even within a given stability class.

a. Empirical relations of the exchange coefficient.

The role of stability in controlling turbulence is demonstrated by the table which shows that a factor of approximately 25 exists between the "stable" and "slightly stable" classes, and the "slightly stable" and "unstable" classes.

Since the source of energy for turbulence in an atmospheric layer bounded at the bottom by a solid surface is the wind shear and the kinetic energy of the wind, a relation might be expected between turbulent mass exchange and wind speed. When the coefficient values are plotted against speed it is shown that, while such a relation does exist, the scatter is great, and that the wind speed is not the dominant control upon the turbulence. A closer relation is obtained if the wind speed is divided by the absolute value of the stability plus one. This has been done and the values are plotted in Figure 24. From the graph it is concluded that the quotient serves as a useful empirical measure of the turbulent exchange to be expected under given stability and wind conditions.

2. *Variation of the exchange coefficient with height.*

Up to this point we have determined values of the exchange coefficient that represent an entire region of the ground layer. This has been done by finding a single value of the mixing ratio gradient for the region. Now with the help of the composite mixing ratio curves, Table V, and the smoothed flow curves, Table IV, presented in Section III, we may investigate the height variations of the exchange coefficient. This has been done by computing gradients from Table V and substituting these averages into the diffusion equation, together with the smoothed average flow for the corresponding height. The values are listed below in Table VIII.

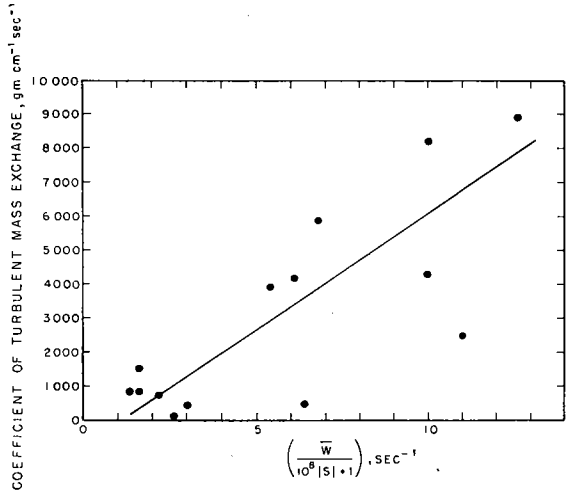

FIG. 24. An empirical wind speed-turbulence relation. The exchange coefficient has been plotted against wind speed divided by 10^8 times the stability plus one.

TABLE VIII

HEIGHT VS. COEFFICIENT OF TURBULENT MASS EXCHANGE

Height % Inversion Height	Gradient $cm^{-1} \times 10^{-9}$	Flow gm $cm^{-1}sec^{-1} \times 10^{-7}$	Coefficient gm $cm^{-1}sec^{-1}$
0	—	135	—
5	26.0	122	480
10	8.0	108	1350
20	6.8	85	1250
40	5.2	52	1000
60	4.1	30	730
80	4.4	16	360
90	20.0	13	65
100	53.0	10	19
110	88.0	8	9.5

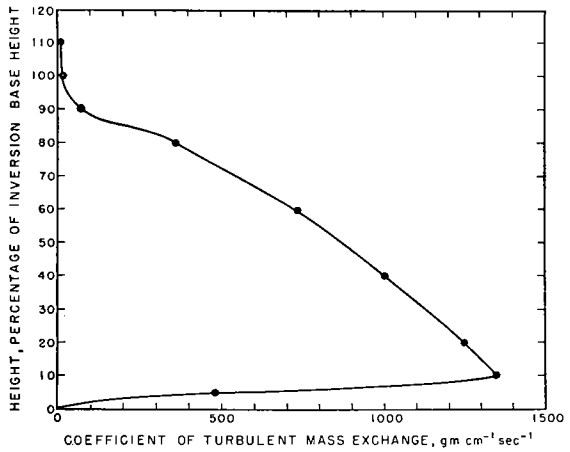

FIG. 25. Coefficient of turbulent mass exchange plotted against height, showing its variation throughout the ground layer.

The Table, and Figure 25, plotted from the Table, show that the coefficient increases rapidly from the molecular value, 3×10^{-4} gm cm^{-1} sec^{-1}, at the surface, to 1350 gm cm^{-1} sec^{-1} at 10% of the inversion height, or about 120 m. The coefficient then decreases slowly to the 80% mark, where it reaches a value of but 360 gm cm^{-1} sec^{-1}. It then drops more rapidly to 19 gm cm^{-1} sec^{-1} at the 100% level. In the inversion it drops to the still lower value of about 10 gm cm^{-1} sec^{-1}.

a. Linear representation of the height variation of the coefficient of turbulent mass exchange.

The problem of the measurement and the functional representation of the variation of the eddy diffusivity with height was studied first by Akerblom (1908). He applied Ekman's expression for the variation of ocean currents to the wind profile of the atmosphere. Both works assumed a constant value of the diffusivity, an assumption now known to apply only to limited regions. Mildner (1932) and Sverdrup (1936) determined values of diffusivity at several heights in the ground layer from balloon observations of the wind velocity. Approximately linear variations of the diffusivity with height were found. Recent studies have been made to evaluate the mass exchange of properties other than momentum. Haurwitz and Stommel (Bunker, et al, 1949) have constructed mixing ratio curves from the sea surface up through the cloud layer of the trade wind region, using constant and linear heights variations of the coefficient of turbulent mass exchange. Craig (1949) finds from a study of the exchange of water vapor that a linear increase in the diffusivity in the lowest meters of air, and a constant value above this, is a satisfactory model for stable air.

Inspection of Table VIII and the investigation of other workers suggests that the height variation of the turbulent mass exchange in the several layers can be represented by linear functions. To check the adequacy of this simple hypothesis a calculation of the mixing ratio values at many heights in the different layers of the lower atmosphere has been carried out using values of A and E, which were constant or linear functions of z in the following equations (7), (8), or (9).

Since it is desired to compute the mixing ratio curve from assumed variations of A_z and E_z, the following expressions are developed:

$$q_z = q_a + \int_a^z \frac{\partial q}{\partial z}\, dz \tag{11}$$

from the diffusion equation (1)

$$\int_a^z \frac{\partial q}{\partial z}\, dz = -\int_a^z \frac{E_z}{A_z} dz \tag{12}$$

so that

$$q_z = q_a - \int_a^z \frac{E_z}{A_z} dz \tag{13}$$

If both E and A are constant throughout a layer then

$$q_z = q_a - \frac{E_a}{A_a}(z)\Big]_a^z \tag{7}$$

This solution defines the mixing ratio curve in layers such as the laminar layer.

In the case with E and A both varying linearly,

$$q_z = q_a - \frac{\lambda z}{\gamma} + \frac{\gamma E_a - \lambda A_a}{\gamma^2} \log (A_a + \gamma z - \gamma a)\Big]_a^z \tag{8}$$

where $A = A_a + \gamma z$, and $E = E_a + \lambda z$.

If E is constant, and A varies linearly, then

$$q_z = q_a - \frac{E_a}{\gamma} \log (A_a + \gamma z - \gamma a)\Big]_a^z \tag{9}$$

The data used for this analysis are from the series obtained over the Gulf of Maine on October 20, 1949. This pair of two soundings has been selected for two reasons. First, transport values were not changing rapidly with time, since the air mass had blown a distance of 180 km (about 5 hours) over water before reaching the area of the first sounding. Second, the ground layer was shallow enough (300 m) to prevent the development of significant convective currents. Values of the flow, the gradient, and the turbulent mass exchange are tabulated for several heights in Table IX. A flow of 1×10^{-7} gm cm^{-2} sec^{-1} through the 450 m surface has been assumed in accordance with the study described in the introduction. This value has been adopted in preference to a determination of the flow from observed values in the advection layer which appears to be very heterogeneous, both horizontally and vertically, with respect to both mixing ratio and temperature.

The synthesis of the mixing ratio curve has been started at the surface of the sea. A value of 13°C, based on the November 7 dip bucket

TABLE IX

MEASURED VALUES OF THE FLOW AND GRADIENT OF WATER VAPOR AND COEFFICIENT OF TURBULENT MASS EXCHANGE GULF OF MAINE—OCTOBER 20, 1949

Surface m	Flow gm cm^{-2} sec^{-1}	Gradient cm^{-1}	Coefficient gm cm^{-1} sec^{-1}
0	2.6 x 10^{-6}	—	—
30	2.4	− 1.25 x 10^{-8}	190
60	2.3	"	185
90	2.2	"	175
165	1.8	"	145
210	1.3	"	105
270	0.89	"	70
300	0.81	− 1.25 x 10^{-8}	56
330	0.42	− 12 x 10^{-8}	3.5
360	0.33	"	2.7
390	0.22	"	1.8
420	0.18	"	1.5
450	0.10 assumed	− 1 x 10^{-8}	10
700	0.10 assumed	− 1 x 10^{-8}	10

temperature of 11.1°C, and on the mean temperature charts, has been adopted as the most probable value of the sea temperature. The saturation vapor pressure of the air in contact with the water is thus about 9.5 gm/kg.

The primary object of the synthesis of the mixing ratio curve is to check the applicability of linear functions to the height-diffusivity relation in 30 m to 450 m region. The curve has been synthesized from the sea surface up, although no observations were taken in the 0–30 m region which can be used as a check on the functions and constants used.

Table X gives the values of the mixing ratio used for the verification of the "correct" choices of γ, which is the rate of change of A, and of λ, which is the rate of change of the water vapor flow, E.

Starting with the laminar sub-layer, the saturation value of the mixing ratio at the sea surface is 9.5 x 10^{-3} gm per gm, and the molecular diffusivity of the air equals 0.245 cm^{-2} sec^{-1} at 13°C, corresponding to an A value of 3 x 10^{-4} gm cm^{-1} sec^{-1}. In this layer, since both the diffusivity and flow are constant, equation (7) applies. This yields a mixing ratio of 8.6 x 10^{-3} at the 10^{-1} cm level, and 7.7 x 10^{-3} at the 2 x 10^{-1} cm level. This rapid falling off of the mixing ratio with distance from the surface cannot extend significantly beyond the 2 x 10^{-1} cm level and allow a gradient that fits the verification curve. This value is twice the thickness usually assigned to the laminar sub-layer.

TABLE X

MIXING RATIO CURVE FOR USE IN VERIFYING SYNTHESIS

Surface m	Mixing Ratio gm/gm	Surface m	Mixing Ratio gm/gm
0	9.5 x 10^{-3}	330	5.8 x 10^{-3}
30	6.1 x 10^{-3}	450	4.3 x 10^{-3}
300	5.8 x 10^{-3}	700	4.0 x 10^{-3}

Using $\lambda = 2 \times 10^{-2}$ in equation (11) a set of mixing ratio values is obtained for the next layer. Since no observations were taken in this layer at the time of the airplane sounding, the verification can be made only by the way in which they join the other layers.

Justification of the application of equation (8) to the 5 m to 30 m region is found by plotting the October 1, 1947, boat observations of mixing ratio in conjunction with the two lowest airplane observations against $-10^{-2} z + \log z$ (Figure 26). This choice of the coefficient of z corresponds to $\lambda = -10^{-10}$, $\gamma = 10^{-2}$, $E = 10^{-5}$, and $A = 10^{2}$, all reasonable approximations of conditions existing in the layer on October 1, 1947. It is seen that all the points fall very close to a straight line from the 4 m to 30 m level.

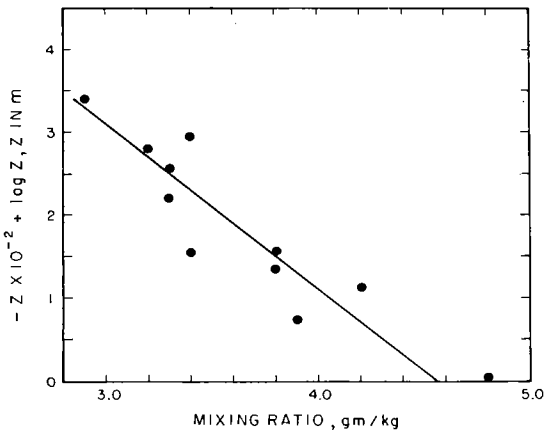

FIG. 26. Mixing ratios in the lowest 30 m observed from a boat October 1, 1947, plotted against $-10^{-2}z + \log z$.

The mixing ratio values in the upper frictional region of the ground layer have been determined directly from the airplane observations, and offer the first chance of a check on the assumption of linear variations of A. The substitution of $\lambda = 6 \times 10^{-11}$ and $\gamma = -5 \times 10^{-3}$ in equation (8) yields a satisfactory fit to the observed mixing ratio values. The coefficient drops from 190 gm cm^{-1} sec^{-1} at 30 m, to 40 gm cm^{-1} sec^{-1} at 330 m.

To continue the computation of the mixing ratio curve into the inversion region it was found

that a discontinuity in the value of A yielded the best fit. The accelerometer traces show an exceedingly rapid decrease in the turbulence of the air in the region. The region is described best as a boundary zone with a steep turbulence gradient, as shown in Figure 24, but penetrated frequently by the gusts from below, so that parcels of air with great turbulence are encountered in smooth air. The observations show large oscillations of the mixing ratio values in the 330 m region, indicative of air parcels penetrating a stable layer.

Above the irregular zone of discontinuity is the region of the temperature inversion. In this region the diffusivity decreases slowly with height from the value of 3.5 gm cm^{-1} sec^{-1} found at the top of the discontinuity, to a value of 0.9 gm cm^{-1} sec^{-1} at 450 m.

In passing from the inversion to the advection layer, a tenfold decrease in the mixing ratio gradient occurs which must be satisfied. If continuity of flow is maintained in this area, then a tenfold increase in the diffusivity is required. This seems reasonable in view of the fact that the top of the inversion is reached at this point, and less stable air is present aloft. In both Tables IX and XI the transition from the inversion region to the advection layer appears as a second discontinuity comparable to the lower one. In fact this is probably not the case. Rather, the increase in the turbulence is more comparable to the slow increase of 10 gm cm^{-1} sec^{-1} in 2 m to 5m above a material surface. In this case, the smooth inversion air takes the place of the surface. The similarity to a discontinuity arises from the inability of the airplane to explore satisfactorily any thin layer in the atmosphere. While the plane is equally incapable of exploring the lower discontinuity, it is believed that a true interface exists between the two air layers.

The height of surfaces, mixing ratios, and coefficients of turbulent mass exchange are summarized in Table XI. Names of layers and regions, and values of λ and γ are given in the first column. The agreement between the mixing ratios entered in Tables IX and X indicates that the simple assumption of a linear variation of the coefficient of turbulent mass exchange in each of several layers is sufficient to account for the observed height distribution of the mixing ratio.

TABLE XI

GRADIENTS AND EXCHANGE COEFFICIENTS SATISFYING MIXING RATIOS OBSERVED OCTOBER 20, 1949

Layers and Gradients cm^{-1}	Height cm	Mixing Ratio gm/kg	Exchange Coefficient gm cm^{-1} sec^{-1}
Laminar sub layer	0	9.5	3×10^{-4}
$\lambda = 0$	10^{-1}	8.6	3×10^{-4}
$\gamma = 0$	2×10^{-1}	7.7	3×10^{-4}
Bottom layer	2×10^{-1}	7.7	3×10^{-4}
	10^{0}	7.2	1.8×10^{-2}
$\lambda = 0$	10^{1}	6.8	1.98×10^{-1}
$\gamma = 2 \times 10^{-2}$	10^{2}	6.5	2
	5×10^{2}	6.3	10
Ground Layer (Bottom frictional region)			
$\lambda = 8 \times 10^{-11}$	5×10^{2}	6.3	10
$\gamma = 7.2 \times 10^{-2}$	10^{3}	6.2	46
	3×10^{3}	6.1	190
Ground Layer (Upper Frictional region)			
$\lambda = 6 \times 10^{-11}$	3×10^{3}	6.1	190
$\gamma = 5 \times 10^{-3}$	10^{4}	6.0	155
	3×10^{4}	5.8	55
	3.3×10^{4}	5.8	40
Ground Layer (Inversion Region)			(Discontinuity in A)
	3.3×10^{4}	5.8	3.5
$\lambda = 2.7 \times 10^{-11}$	4×10^{4}	4.8	2.0
$\gamma = 2.2 \times 10^{-4}$	4.5×10^{4}	4.3	0.9
Advection Layer			
$\lambda = 0$	4.5×10^{4}	4.3	10.0
$\gamma = 0$	7×10^{4}	4.0	10.0

3. *Relative transport by diffusion and free-convection.*

The coefficients of turbulent mass exchange discussed in the previous section were computed without regard to the process by which the accumulation of water vapor in the ground layer was accomplished. It is questionable whether coefficients so determined describe a process which corresponds to the basic notion of unordered turbulent motion of a fluid. The question arises since the presence of free-convective currents is detected frequently within the turbulent stream. Such convective currents extending from the lowest regions of the ground layer to the base of the inversion can transport greater amounts of water vapor than can the smaller scale turbulent eddies. Substituting a transport value partially due to convection into the diffusion equation yields a coefficient much too large to describe the smaller scale turbulent transport. To determine a value of the coefficient that conforms to the notion of unordered turbulent eddies that must be treated statistically, rather than to the notion of larger, systematic motions that can be treated specifically in detail, such as convection cells, thunderstorms,

and cyclones, the transport of vapor by convection must be separated from the total transport.

Not all meteorologists will consider this separation a necessary or even desirable step, since free-convection may be considered as simply another turbulent phenomenon. This point of view leads to the acceptance of the previously computed coefficients as a valid measure of the turbulent intensity of the atmosphere. The author, however, prefers to consider free convection as a process differing from turbulence, and indeed, is forced into this position by the occurrence of net upward fluxes of water vapor in the face of positive gradients of the mixing ratio. Thus a situation is created in which the net transport can no longer be expressed in terms of a geometric distribution of vapor and the degree of turbulence. A separation of the transport by diffusion from the transport by convection is clearly necessary in this case.

The problem of separation resolves itself into the evaluation of the ability of the currents to transport water vapor. A re-evaluation of the turbulent mass exchange must be made in the light of the study of five series of soundings which show evidence of free-convection currents. These series offer the chance of estimating the transports by convection, and allow a truer determination of the coefficient of turbulent mass exchange.

The vertical transport of water vapor through a surface can be expressed in terms of eddy diffusion and convective transport by the following equation:

$$ES = (-A\partial q/\partial z)(S - S') + \rho w'\Delta q S' - \rho w^2(\partial q/\partial z)(S - S')t \qquad (14)$$

where S is the total unit area; S′ the area occupied by convective up drafts; w′ the average convective velocity; w the average rate of subsidence compensating the upward velocities; Δq the difference in mixing ratio between the convecting air and its surroundings, and t the unit time interval.

The successful application of equation (14) depends primarily on the reliability of the determinations of w′, the velocity of the ascending air. No direct measurement of the velocity has been made. The values to be substituted in the equation are estimates based on the indirect measurements and relations. These estimated values may be in error by a factor of two or more, but it is believed that the order of magnitude is correct.

One estimate of the convective velocities can be made from the gust velocities. An upper limit to the convective velocities can be assigned from an inspection of Figure 23 which shows maximum gust velocities of 1.4–1.6 m/sec in the 900–1200 m region, where the buoyant air parcels will reach their greatest velocities just prior to entry into the inversion. Even higher gust velocities exist below the 600 m level, where convective currents are relatively weak, but these gusts are produced primarily by the turbulence alone. Converting effective gust velocities to true gust velocities by increasing them by 50% (Rhode, 1937), we find a maximum velocity of 2.2 m/sec at the highest level. On January 17, 1950, the plane was flown through a small but active cumulus cloud at 1500 m. The accelerometer registered an acceleration of 0.36 g, corresponding to an effective gust velocity of 2.0 m/sec, and a true vertical gust velocity of about 3.0 m/sec. Assuming that the findings of Moskovitz (1945), that gust velocities are equal to the updrafts in convective-type clouds, also applies to convective currents of non-saturated air in a turbulent stream, then 2.2 m/sec and 3.0 m/sec are the maximum updrafts a convecting parcel will attain upon reaching the 1000 m and 1500 m level. Velocities at lower levels may be approximated by linear interpolation between these values and zero velocity at the surface, or by the use of curves such as are integrated by Houghton and Cramer (1951).

Lower limits to the average velocity may be established in a few cases by determining the rate of ascent of a particular parcel from an estimate of the point of departure from the surface. The distance to the previous upwind sounding had to be chosen as the departure point in studying the cases of convection near shore. Treating the moist parcel observed at 600 m (shown in Figure 11) on October 1, 1947, in this manner, the minimum average value is 0.55 m/sec. The 1.1 m/sec attained at the 600 m level may be compared with the 2.2 m/sec at the 1000 m level determined in the preceding paragraph.

The cloud that developed in the helix of ascent of the sounding aircraft 12 km downwind on September 1, 1948, is particularly well suited for estimating its ascension rate, because the parcel must have received its final heating from the land surface. This conclusion follows from the fact that the water was cooler than the solar radiation

heated land, and nearly in thermal equilibrium with the main body of air in the ground layer. As the air mass moved out over the water, the lowest 50 to 100 m of air cooled a few tenths of a degree until the entire column was in neutral equilibrium. The few tenths of sky coverage by cumulus clouds over the land disappeared beyond the second sounding so that no low clouds occurred in the area of the final sounding. From these observations it is concluded that the cloud observed 12 km downwind received the necessary heat to make it buoyant from contact with the heated ground. The ascent of 1700 m in the 1100 seconds required to travel 12 km corresponds to an average velocity of 1.5 m/sec. During the last 200 m of its ascent the parcel was being decelerated by the stability of the inversion region. Its average velocity through the turbulent regions is then 1.8 m/sec. As mentioned earlier this value is not an exact determination but is intended to establish the order of magnitude of convective currents that have continuity throughout the ground layer. Day to day variations of the average velocity will occur. It is probable that many other buoyant parcels of smaller size exist with lower velocities that never reach the inversion region. Transport by parcels with these sizes and velocities has been treated by Priestley and Swinbank (1947). In the estimate of transport by convection that follows, the effect of these smaller parcels is not considered.

An estimate of the convective transport of water vapor on October 1, 1947, through the 600 m surface, has been based on a velocity of 1.1 m/sec, a convective area, S′, of 0.1, and a mixing ratio difference of 1×10^{-3} gm/gm. The transport is 13×10^{-6} gm cm^{-2} sec^{-1}. This flow represents 33% of the flow through the 200 m surface, and 80% through the 600 m surface.

The estimate of the convective flow through the 1300 m surface on September 1, 1948, is found to be 6×10^{-6} gm cm^{-2} sec^{-1} when Δq is 0.2×10^{-3} gm/gm, S′ is 0.1, and w′ is 260 cm sec^{-1}. A flow of 6×10^{-6} gm cm^{-2} sec^{-1} is 14% of the flow through the 200 m surface. A convective area of 0.1 is used in spite of 0.2 sky coverage by cumulus, as it was considered that at least half of the cumulus were inactive, that is, brought to rest or even sinking back into the mixed layer.

In applying equation (14) to the case of February 3, 1950, it must be recognized that a basic change in the transport has occurred during the passage of the air from land to the final sounding area. This change may be demonstrated by computing the correlation between the turbulence index and the potential temperature or mixing ratio. The author (1952) has shown that the presence of convective currents within a turbulent stream can be detected by statistical treatment of the flight records of an airplane flying through the air. Ten second averages of the turbulence index and temperature are found to have significantly high correlation coefficients whenever convection is present in the stream. The correlation exists between either temperature or mixing ratio and turbulence when the air passes over warm water surfaces.

Correlations have been computed from the February 3, 1950, data to recognize the presence of convective currents in the ground layer. Mixing ratio-turbulence index correlations have been computed for each 300 m slice of the ground layer. Every height for which simultaneous values of the mixing ratio and the index were available, a total of 90 pairs of observations, were used in the determination. Similarly, correlations were computed from pairs of potential temperatures and turbulence indices for several height ranges both over the land and over the water. The values are tabulated in Table XII.

TABLE XII

CORRELATION COEFFICIENTS, FEBRUARY 3, 1950

Over land at Portland, Maine		Over waters of Gulf of Maine (42° 35′N, 69° 30′ W)			
Height m	Coefficient (Temp.-Turb. I.)	Height m	Coefficient (Temp.-Turb. I.)	Height m	Coefficient (Mix.R.-Turb. I.)
120–610	0.6	210–610	0.0	150–300	0.1
640–1220	0.3	640–1220	0.7	300–600	0.3
1250–1520	− 0.2	1250–1610	− 0.5	600–900	0.6
1580–1830	− 0.3			900–1200	0.5
				1200–1500	0.4

The high value of 0.6 in the lowest layer over the land indicates that gusts of convective air from the heated land were present in this layer. The correlation diminishes above the 600 m level, showing that the convecting parcels do not persist to this height. By contrast, over the water no convective activity is present in the lowest layers, but becomes significant above the 600 m level. The change in predominating method of transport of heat and water vapor may be summarized

as follows. As the air moved over the water, transport of water vapor by diffusion was first greatly increased as the gradient in the lower layers increased. Later, convective currents in the upper region of the ground layer were created so that 20 km offshore a few small puffs of cumulus were observed. Once the convective currents were established in the upper region, a more direct transport process was set up which moved water vapor from the lower region to the inversion. As the air progressed further offshore this method of transport increased, causing accumulations of moist air at the base of the inversion. Continuation of this process reduced the mixing ratio gradient in the upper region, so that the transport by diffusion diminished. By the time the air arrived 150 km offshore, the sense of the vertical diffusion had been reversed due to the development of a positive gradient. In the lower region transport by diffusion continued, since the gradient remained negative.

An evaluation of the relative transports by diffusion and convection can be made from the observations and the convective velocities estimated in the previous discussion. The value of 2 m/sec is accepted here as a fair estimate of the speed that a rising parcel of non-saturated air will attain upon reaching the 1200–1500 m region. The values of the relative areas of convective activity are based on the observed sky coverage of 3/10. It is assumed that all rising parcels will become saturated and thus visible in the last 50–100 meters of their ascent. Since the ascending parcels are brought to rest by the stable inversion air, and finally forced down into the upper region again, 1/10 is accepted as the best estimate of the relative area of active, upward moving parcels at the inversion level. The relative areas, which are time averages, at lower levels will be larger, since the parcels will be moving slower. The difference in mixing ratio between the connecting parcels and the surrounding air decreases with height, due to the positive gradient. A check on the reasonableness of these estimated values may be made by comparing them with the observed flow through the 500 m surface. It was observed that a net upward flow of 300 gm cm^{-2} sec^{-1} occurred through this surface, while the estimate of convective flow gives 380 gm cm^{-2} sec^{-1}. As a positive gradient exists at this level, convective currents must transport all of the 300 gm cm^{-2} sec^{-1}, plus an additional amount to compensate the downward flow by diffusion. Another check, but one which is not met so successfully, is the height variation of the coefficient of turbulent mass exchange. The height increase of the coefficient indicates that either the estimates of the convective elements contain an error, or the small moisture gradients have not been determined sufficiently accurately. A third possibility is that the energy of the rising air parcels is transferred into turbulent energy, thus increasing the exchange coefficient. The complete set of observed and computed values are entered in Table XIII. Column 1 gives the heights of the surfaces in question. Column 2 gives the net observed flow through the surface, averaged over the trajectory from 15 km to 130 km downwind. Average values over the first 15 km of water on other days were used in computing the entered

TABLE XIII

SEPARATION OF TRANSPORT OF WATER VAPOR BY TURBULENCE AND CONVECTION

Height of Surface m	Observed Flow through Surface gm cm^{-2} sec^{-1}	Accumulation in Layer gm cm^{-2} sec^{-1}	Vertical Velocity cm sec^{-1}	Relative Convective Area	Mixing Ratio Difference gm/gm
0	420×10^{-8}	20×10^{-8}	....	....	....
100	400×10^{-8}	100×10^{-8}	....	....	....
500	300×10^{-8}	190×10^{-8}	75	0.27	1.5×10^{-4}
1000	110×10^{-8}	75×10^{-8}	150	0.13	1.0×10^{-4}
1360	35×10^{-8}	35×10^{-8}	200	0.10	0.5×10^{-4}

Height of Surface m	Convective Transport gm cm^{-2} sec^{-1}	Diffusive Transport gm cm^{-2} sec^{-1}	Mixing Ratio Gradient cm^{-1}	Coefficient of Turbulent Mass Exchange gm cm^{-1} sec^{-1}
0	0	420×10^{-8} up	....	....
100	?	400×10^{-8} up	-5×10^{-9}	800
500	380	80×10^{-8} down	0.5×10^{-9}	1600
1000	230	120×10^{-8} down	0.5×10^{-9}	2400
1360	115 90*	10×10^{-8} up	-30×10^{-9}	3

* Return transport due to parcels falling back into turbulent air.

values. The accumulation of water vapor in each layer is entered in Column 3. Colums 4, 5, and 6 present the vertical velocities, relative areas, and mixing ratio differences already discussed. The convective transport computed from these values is given in Column 7. The value of 90, labelled *return*, represents the estimate of the amount of water vapor returned as the air is forced back down into the layer. Column 8 gives the transport by diffusion required to balance the observed flow and the convective flow. Columns 9 and 10 give the observed gradients of the mixing ratio and the computed coefficient of turbulent mass exchange. Some doubt is placed on the exact values as they do not agree with the height distribution described previously. The value found at the 500 m level may be too low, due to a poor determination of the gradient at this level. The gradient may be smaller than 5×10^{-10} cm^{-1}, since it is near the transition from the negative to the positive gradient.

The flow of water vapor produced by the subsidence compensating the upward convective currents was found to be negligible (10^{-11} gm cm^{-2} sec^{-1}) and has not been considered in evaluating equation (14).

As an aid in visualizing the water vapor transport, the values of accumulation, convective flow, and transport of water vapor by diffusion, have been entered in Figure 27. The transport processes operating 100 km downwind over the Gulf of Maine may be summarized briefly as: (1) an

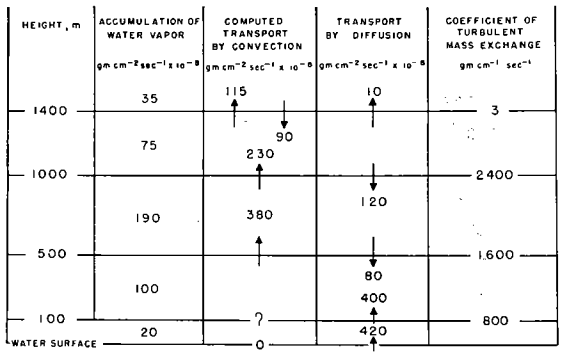

FIG. 27. Budget diagram of transport of water vapor by turbulence and convection in the air over the Gulf of Maine.

upward transport of water vapor by diffusion in the lowest 100 m, (2) large upward transport by convection in the 100 m to inversion base region with a downward transport by diffusion, (3) an upward convective transport through the inversion base with a return flow due to the parcels falling back to an equilibrium position, and a small upward flow through the inversion by diffusion.

V. SUMMARY

Temperature, humidity, and roughness measurements have been made from an airplane flying through the ground layer of continental air blowing over warmer water. The soundings extended up through the well-mixed, turbulent ground layer, usually 1200 m thick, and through the sharp inversion which separates the ground layer from the more stable atmosphere above it.

From a series of soundings taken at increasing downwind distances up to 150 km from shore, the accumulation of water vapor trapped beneath the inversion is determined. The flow of water vapor through unit horizontal surfaces at the water surface and at 200 m is found to vary within the ranges, 2.6×10^{-6} to 91×10^{-6} gm cm^{-2} sec^{-1}, and 0.9×10^{-6} to 43×10^{-6} gm cm^{-2} sec^{-1}.

Mixing ratio gradients have been determined to lie within the wide range -60×10^{-9} to 0.0×10^{-9} cm^{-1} in the bottom frictional region over the water and in the smaller range of -24×10^{-9} cm^{-1} to $+1.0 \times 10^{-9}$ cm^{-1} in the upper frictional region over the water.

Since the relation between the transport of a property and the geometrical distribution of the property is expressed best by the diffusion equation, $E = -A\frac{\partial q}{\partial z}$, the determined values of the gradient and flow have been substituted in this equation. The resulting values of the coefficient of turbulent mass exchange lie within the range 68 to 15,000 gm cm^{-1} sec^{-1}. It is shown that while the stability of the air mass exerts a control on turbulence, wide ranges of the coefficient, 68 to 2500 gm cm^{-1} sec^{-1} in the slightly stable range, and 780 to 15,000 gm cm^{-1} sec^{-1} in the neutral or unstable range, exist within a given stability range. The wind speed divided by one plus the absolute value of the stability is shown to be a fair empirical measure of the coefficient. In the vertical direction, an average coefficient, determined from smoothed gradient and flow curves, increases from the molecular values of diffusivity at the water surface to a maximum value of 1350 gm cm^{-1} sec^{-1} at 10% of the height of the ground layer inversion. It decreases slowly to a value of 100 gm cm^{-1} sec^{-1} at 88% of the inversion height. Through the inversion the coefficient drops to the low value of 1 to 10 gm cm^{-1} sec^{-1}. The linear representation of the variation of the coefficient in each of the many sub-divisions of the ground layer is tested and found to be a good approximation.

The influence of free-convection, here considered as a process distinct from eddy diffusion, on the transport of water vapor, is recognized and evaluated. It is shown that the upward transport by diffusion may be reversed in the few hundred meters below the base of a strong inversion. This reversal results from the production of a positive mixing ratio gradient below the inversion base by the sudden halting of the moist convective currents which build up the moisture concentration above the concentration reached at the intermediate levels.

REFERENCES

Åkerblom, F. A.

1908 Recherches sur les courants les plus bas de l'atmosphère au dessus de Paris. *Nova Acto Reg. Soc. Sci. Upsalla*, Sec. 4, Vol. 2, p. 2.

Army Air Forces Weather Service

1945 Aircraft Weather Reconnaissance. *AAF Weather Service Manual*, 105–128–I, 218 pp.

Berry, F. A., E. Bollay and N. R. Beers

1945 Handbook of Meteorology. McGraw-Hill Book Co., New York. 1068 pp., numerous text figs.

Bunker, A. F.

1952 Recognition of the presence of convective currents within a non-saturated turbulent layer of the atmosphere. Symposium on atmospheric turbulence in the boundary layer. Dept. of Meteorol., Mass. Inst. Tech. and Geophys. Res. Dir., AF Cambridge Res. Lab. In press.

Bunker, A. F., B. Haurwitz, J. S. Malkus, and H. Stommel

1949 Vertical distribution of temperature and humidity over the Caribbean Sea. *Pap. Phys. Oceanogr. and Meteorol.*, Vol. 11, No. 1, 82 pp.

Burke, C. J.

1945 Transformation of polar continental air to polar maritime air. *Jour. Meteorol.*, Vol. 2, No. 2, pp. 94–112.

Craig, R. A.

1946 Measurements of temperature and humidity in the lowest 1000 feet of the atmosphere over Massachusetts Bay. *Pap. Phys. Oceanogr. and Meteorol.*, Vol. 10, No. 1, 47 pp.

1949 Vertical eddy transfer of heat and water vapor in stable air. *Jour. Meteorol.*, Vol. 6, No. 2, pp. 123–133.

Craig, R. A., and R. B. Montgomery

1949 Evaporation (measured) from ocean into hydrostatically stable air. *Jour. Meteorol.*, Vol. 6, No. 6, pp. 426–427.

Dalton, J.

1802 Experimental essays on the constitution of mixed gases; on the force of steam of vapor from water and other liquids in different temperatures, both in a Torricellian vacuum and in air; on evaporation, and on the expansion of gases by heat. *Mem. Lit. and Phil. Soc. of Manchester*, Vol. 5, pp. 535–602.

Dryden, H. L.

1943 A review of the statistical theory of turbulence. *Quart. Appl. Math.*, Vol. 1, pp. 7–42.

Ertel, H.

1930 Eine Methode zur Berechnung des Austauschkoeffizienten aus den Feinregistrierungen der turbulenten Schwankungen. *Gerlands Beitr.*, Vol. 25, pp. 279–289.

Flohn, H., and R. Penndorf

1950 The stratification of the atmosphere. *Bull. Amer. Meteorol. Soc.*, Vol. 31, Nos. 3, 4, pp. 71–78, pp. 126–130.

Hewson, E. W.

1936 The application of the wet-bulb potential temperature to air mass analysis. I. *Quart. Jour. Roy. Meteorol. Soc.*, Vol. 62, pp. 387–420.

1938 The application of the wet-bulk potential temperature to air mass analysis. IV. *Quart. Jour. Roy. Meteorol. Soc.*, Vol. 64, pp. 407–418.

Houghton, H. G., and H. E. Cramer

1951 A theory of entrainment in convective currents. *Jour. Meteorol.*, Vol. 8, No. 2, pp. 95–102.

Huss, P. O., and D. J. Portman

1948 Study of natural wind and computation

1949 of the austausch turbulence constant. *Daniel Guggenheim Air. Inst. Rep.*, Nos. 149 and 156, 38 pp. and 49 pp., numerous figures. Manuscript reports to the Office of Naval Research.

JAW, J.
1937 Zur Thermodynamic der Passat-Grundströmung. *Veröff. der Meteorol. Inst. der Univ. Berlin*, Bd. 2, Heft 6, pp. 1–24.

KATZ, I.
1947 An airplane psychrograph. *Bull. Amer. Meteorol. Soc.*, Vol. 28, No. 8, pp. 363–370.

LETTAU, H.
1937 Weiterführung der Freiballon-Untersuchungen über effectiven Vertikalaustausch und Luftmassen-Alterung mit Anwendug auf die Frage der Land-Verdunstung. *Meteorol. Zeitz.*, Bd. 57, pp. 406–412.

MIDDLETON, W. E. K.
1942 Meteorological Instruments. Univ. of Toronto Press, Toronto. 213 pp., 160 figs.

MILDNER, P.
1932 Über die Reibung in einer speziellen Luftmasse indem unteresten Schichten der Atmosphäre. *Beitr. Phys. Atm.*, Vol. 19, pp. 151–158.

MONTGOMERY, R. B.
1940 Observations of vertical humidity distribution above the ocean surface and their relation to evaporation. *Pap. Phys. Oceanogr. and Meteorol.*, Vol. 7, No. 4, 30 pp.

MOSKOVITZ, A. I.
1945 Characteristics of vertical drafts and associated vertical-gust velocities within convective-type clouds. *Nat. Advis. Com. Aero.* RB L_5AO_3, 9 pp.

PETTERSSEN, S.
1940 Weather analysis and forecasting. McGraw-Hill Book Co., New York. 505 pp. 249 figs.

PRIESTLY, C. H. B., and W. C. SWINBANK
1947 Vertical transport of heat by turbulence in the atmosphere. *Proc. Roy. Soc.*, Ser. A, Vol. 189, pp. 543–561.

RHODE, R. V.
1937 Gust loads on airplanes. *Soc. Auto. Eng. Trans.*, Vol. 32, pp. 81–88.

RIEHL, H., T. C. YEH, J. S. MALKUS, and M. E. LASEUR
1951 The north-east trade of the Pacific Ocean. *Quart. Jour. Meteorol. Soc.*, Vol. 77, No. 334, pp. 598–626.

ROSSBY, C.-G., and R. B. MONTGOMERY
1935 The layer of frictional influence in wind and ocean currents. *Pap. Phys. Oceanogr. and Meteorol.*, Vol. 3, No. 3, 101 pp.

SCHNEIDER-CARIUS, K.
1947 Der Schichtenbau der Troposphäre. *Meteorol. Rundsch.*, Vol. 1, pp. 79–83.
1947*a* Der Aufbau der Grundschicht in Mitteleuropäischen Klimiagebiet. *Meteorol. Rundsch.*, Vol. 1, pp. 228–231.

SMITHSONIAN INSTITUTION
1939 Smithsonian meteorological tables. *Smithsonian Misc. Collections*, Vol. 86 (whole volume). Fifth Revised ed., 282 pp.

SPILHAUS, A. F.
1938 A bathythermograph. *Jour. Mar. Res.*, Vol. 1, No. 2, pp. 95–100.

SVERDRUP, H. U.
1936 The eddy conductivity of the air over a smooth snow field. *Geofys. Publ.*, Vol. 11, No. 7, 69 pp.
1937 On the evaporation from the oceans. *Jour. Mar. Res.*, Vol. 1, No. 1, pp. 3–14.

TAYLOR, G. I.
1915 Eddy Motion in the atmosphere. *Phil. Trans. Roy. Soc.*, A, Vol. 215, pp. 1–26.

THORNTHWAITE, C. W., and B. HOLZMAN
1942 Measurement of evaporation from land and water surfaces. U. S. Dep. of Agric., *Tech. Bull.*, No. 817, 143 pp.

WOOD, F. B.
1937 The formation and dissipation of stratus clouds beneath turbulence inversions. *Mass. Inst. Tech. Professional Notes*, No. 10, 27 pp.